Earth-Science Reviews 97 (2009) 44–58

Contents lists available at ScienceDirect

Earth-Science Reviews

journal homepage: www.elsevier.com/locate/earscirev

Thermodynamic model for uplift and deflation episodes (bradyseism) associated with magmatic–hydrothermal activity at the Campi Flegrei (Italy)

Annamaria Lima [a,*], Benedetto De Vivo [a], Frank J. Spera [b], Robert J. Bodnar [c], Alfonsa Milia [d], Concettina Nunziata [a], Harvey E. Belkin [e], Claudia Cannatelli [a,b]

[a] Dipartimento di Scienze della Terra, Università di Napoli Federico II, Via Mezzocannone 8, 80134 Napoli, Italy
[b] Department of Earth Science, University of California Santa Barbara, Santa Barbara, CA 93106, USA
[c] Department of Geosciences, Virginia Tech, Blacksburg, VA 24061, USA
[d] Istituto Ambiente Marino Costiero, CNR, Calata Porta di Massa, Porto di Napoli 80133, Italy
[e] U. S. Geological Survey, 956 National Center, Reston, VA 20192, USA

ARTICLE INFO

Article history:
Received 22 June 2009
Accepted 1 October 2009
Available online 14 October 2009

Keywords:
Bradyseism
Campi Flegrei
Ground deformation
Magmatic–hydrothermal activity
Thermodynamic modelling

ABSTRACT

Campi Flegrei (CF) is a large volcanic complex located west of the city of Naples, Italy. Repeated episodes of bradyseism (slow vertical ground movement) near the town of Pozzuoli have been documented since Roman times. Bradyseismic events are interpreted as the consequence of aqueous fluid exsolution during magma solidification on a slow timescale (10^3–10^4 yr) superimposed upon a shorter (1–10 yr) timescale for the episodic expulsion of fluid from a deep (~3–5 km) lithostatically-pressured low-permeability reservoir to an overlying hydrostatic reservoir. Cycles of inflation and deflation occur during short duration transient events when connectivity is established between deep and shallow hydrothermal reservoirs. The total seismic energy released (4×10^{13} J) during the 1983–1984 bradyseismic crisis is consistent with the observed volume change (uplift) and consistent with the notion that seismic failure occurs in response to the shear stress release induced by volume change. Fluid transport and concomitant propagation of hydrofractures as fluid expands from lithostatic to hydrostatic pressure during decompression leads to ground surface displacement. Fluid decompression occurs along the fluid isenthalp (Joule–Thompson expansion) during transient periods of reservoir connectivity and leads to mineral precipitation. Each kilogram of fluid precipitates about 3×10^{-3} kg of silica along a typical decompression path along the isenthalp. Mineral precipitation modifies the permeability and acts to reseal connection paths thereby isolating lithostatic and hydrostatic reservoirs ending one bradyseism phase and beginning another. Crystallization and exsolution of the magmatic fluid generates $\approx7\times10^{15}$ J of mechanical ($P\Delta V$) energy, and this is sufficient to accomplish the observed uplift at CF. Although magma emplacement is the ultimate origin of bradyseism, fresh recharge of magma is not a prerequisite. Instead, short to intermediate timescale phenomena associated with fluid decompression and expansion in the crust with large variations in permeability, including permeability anisotropy, are the key elements at CF.

Contents

* Corresponding author. Tel.: +39 0812535058; fax: +39 0812535061.
E-mail addresses: anlima@unina.it (A. Lima), bdevivo@unina.it (B. De Vivo), spera@geol.ucsb.edu (F.J. Spera), rjb@vt.edu (R.J. Bodnar), alfonsa.milia@iamc.cnr.it (A. Milia), conunzia@unina.it (C. Nunziata), hbelkin@usgs.gov (H.E. Belkin), claudiac@vt.edu (C. Cannatelli).

0012-8252/$ – see front matter © 2009 Elsevier B.V. All rights reserved.
doi:10.1016/j.earscirev.2009.10.001

1. Introduction

Volcanism and hydrothermal activity at Campi Flegrei (CF) has been active over the past several hundred thousand years and is associated with Quaternary extension along the Eastern Tyrrhenian margin (Milia and Torrente, 1999, 2003) (Fig. 1). Although this region has been the target of intense research, the origin of the volcanism and the geodynamic framework remain a matter of spirited debate (Wortel and Spakman, 2000; Faccenna et al., 2001; Sartori, 2003; Goes et al., 2004; Turco et al., 2006). Approximately three million people reside in the greater Naples area, representing one of the most densely populated volcanically active regions on Earth. Of particular interest regarding volcanic, seismic and geodetic hazards in this region is the phenomenon of slow, vertical ground movements-referred to as bradyseism — that have affected CF since before Roman times (Parascandola, 1947). Bradyseismic ground deformation cycles of inflation (uplift) and deflation (subsidence), collectively referred to as Ground Surface Deformation (hereafter GSD), are especially well documented at CF due to its coastal location and long history of habitation and construction. In particular, the town of Pozzuoli contains three marble columns in the Serapis Temple with boreholes made by marine mollusks (*Lithodamus lithophagus*) occurring at heights ~7 m on the columns (Parascandola, 1947). This represents spectacular evidence for the magnitude of bradyseism at CF within the past few thousand years.

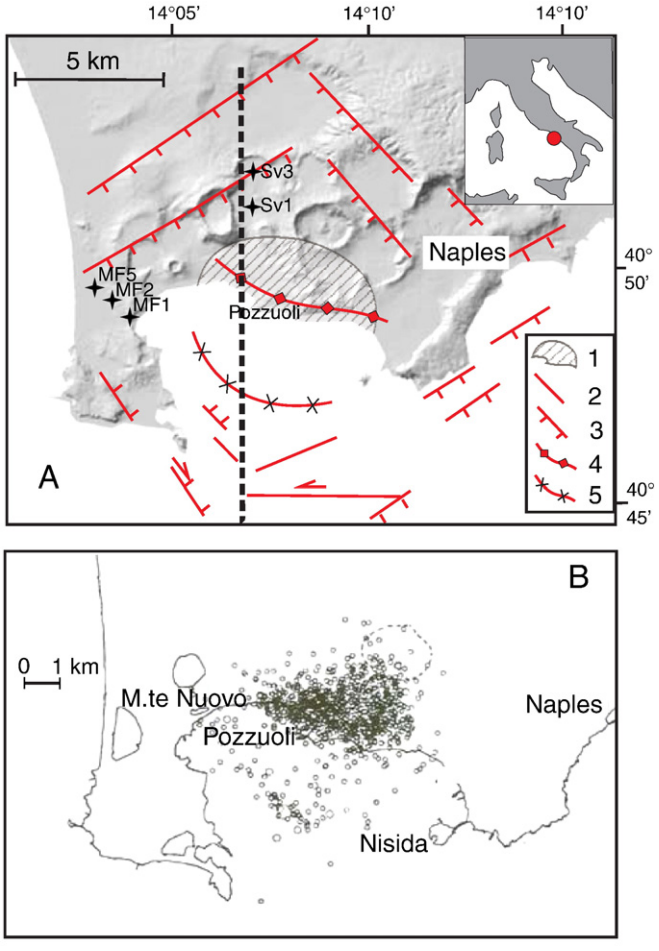

Fig. 1. A. Structural map of the Campi Flegrei–Pozzuoli Bay area (from Milia and Torrente, 2000; Milia et al., 2003). 1. Area affected by an uplift of 100–50% during the 1982–84 bradyseism; 2. Fractures and lateral faults; 3. Normal faults; 4. Pozzuoli anticline; 5. Pozzuoli Bay syncline. Black stars indicate the location of deep geothermal wells (Mofete — MF1, MF2, MF5, and San Vito — SV1, SV3). The dashed line is the location of the geologic cross section shown in Fig. 3. B. Epicenter locations of the earthquakes in the period 1983–84, recorded by 8 stations of the Vesuvius Observatory.

Geodetic methods have been used to establish sub-annual to decadal displacements that include +1.7 m (uplift) during the period 1969–1972, −0.2 m (subsidence) during 1972–1975, +1.8 m in the period 1982–1984 followed by −0.2 m from 1985 to 1988, and +0.13 m of uplift in the period 1988–1989. The general subsidence phase after 1988 has been interrupted by minor, short duration uplifts in 1989, 1994 and 2000. In August 2000, subsidence renewed and stopped in November 2004 with the onset of a new uplift episode, reaching a level of about 4 cm by the end of October 2006 (Troise et al., 2007). These episodes as well as earlier ones are depicted schematically on Fig. 2. The spatial distribution of ground movement at CF, with its sub circular symmetry, is shown in Fig. 1. Ground surface deformation has continued to the present day (e.g., Trasatti et al., 2008). Ground deformation during the earlier period 1450–1538 A.D. culminated with the eruption of Monte Nuovo. This is the only known example at CF when bradyseism preceded a volcanic eruption. Additional bradyseismic events occurred in the CF region before 1538 although ground movement data are not available (Parascandola, 1947; Morhange et al., 2006).

Various models have been proposed to explain the uplift at CF. Because different models have significantly different implications for geohazards and volcanic risk, it is important to examine them closely. For example, if bradyseism requires an input of fresh magma to the magma body, one might anticipate an eruption following a period of uplift. Based on such a model, 30,000 people were evacuated from Pozzuoli during October 1983 and relocated to Monte Ruscello about 3 km away during the 1982–1984 uplift and increased seismicity associated with shallow earthquakes (4 km depth). However, an eruption did not occur either before or after the earthquake swarms and this has led to uncertainty regarding the nature of precautionary civil defence measures imposed to safeguard the population during future events. Improvement in bradyseism forecasting and development of a better conceptual model is clearly relevant to an informed civil defence response involving the safety of millions of inhabitants in the greater Naples area.

Models of CF bradyseism and, indeed, bradyseism worldwide, fall into three main categories. All models ultimately depend on the presence of a magma body at depth but the role of magma in driving bradyseism is quite different. One scenario relates ground surface deformation (GSD) directly to emplacement of a fresh batch of magma at shallow depth. In this model GSD is the response of the crust acting as an elastic or viscoelastic medium into which magma has been emplaced. There are variations on this theme but the central aspect is that intrusion of magma into the crust or a pre-existing magma body drives GSD (e.g., Mogi, 1958). A second class of models also involves fresh magma input (recharge) to trigger bradyseism and views GSD, not in response to pressurized magma, but rather due to the injection of magmatic fluids into overlying crust. Injection of high-temperature magmatic fluid into the shallow hydrothermal reservoir system induces fluid overpressures that may cause the host rocks to inflate depending on the mechanical properties of the local crust (Fournier, 1999). In this model, subsidence results from a decrease in

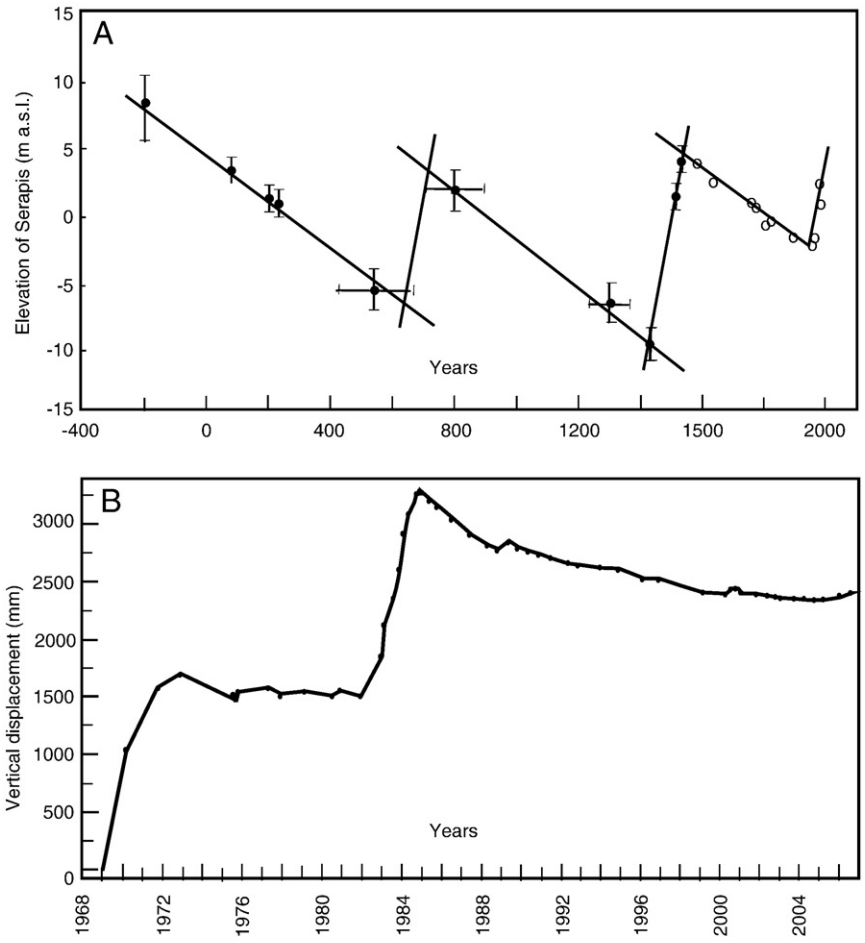

Fig. 2. A. Schematic vertical movements history at Serapis Temple in Pozzuoli. Black circles represent the constraints found from radiocarbon and archaeological measurements by Bellucci et al. (2006); white circles (post-1538) represent inference from Dvorak and Mastrolorenzo (1991). B. Vertical ground displacements as recorded at Pozzuoli Harbour by levelling data in the period 1969–2006 (Macedonio and Tammaro, 2005; Del Gaudio et al., 2005; Pingue et al., 2006).

the flux of magmatic fluid entering the hydrothermal system or as a response to rapid permeability increases and hence pore pressure decreases that occur when the fluid pressure exceeds the local strength of the crustal host, a condition generally easily achieved at shallow depths. The third class of models, the one advocated here (De Vivo and Lima, 2006; Bodnar et al., 2007), differs from previous ones in that magma recharge immediately preceding bradyseism is not a prerequisite condition. Instead, bradyseism results from the complex interplay of two dominant processes operating on very different timescales. The long (10^3–10^4 yr) timescale process is associated with quasi-steady cooling and crystallization of magma at shallow depth and concomitant generation of magmatic fluids by second boiling due to crystallization in a magma body of waning enthalpy. Bradyseism in this model is due to the episodic expulsion of geopressured magmatic fluids into an overlying hydrostatically pressured hydrothermal system. In this case, GSD is caused by the expansion of fluid during short (intradecadal) periods when a connectivity of fluid pathways transiently develops between the two reservoirs (lithostatic and hydrostatic). The timescale of the episodic expulsion process depends on the rate of generation of magmatic volatiles (a background quasi-steady process) and most significantly on the anisotropy, magnitude and temporal variations of the permeability field characterizing the hydrothermal system. At CF there is an overall permeability structure imposed from the sedimentary and metasedimentary rocks of the crust in which, with increasing depth, the ordering is permeable to impermeable back to permeable and then in the deepest part of the system (~5 km) impermeable (contact metamorphic rocks). Of special significance are the low permeability fine grained Middle Pleistocene marine claystones and siltstones at about 2 km depth that make up Unit B (Fig. 3). In the model we propose, the time scale for permeability change is measured in months to years and is modulated by feedback between brittle failure and precipitation reactions superimposed on the inherently anisotropic regional scale permeability imposed by sedimentary structures. Unit B acts as the throttling valve between the hydrothermal and the intermediate lithostatic–hydrostatic reservoirs with distinct vertical gradients in fluid pressure.

In this study we extend the contributions of De Vivo and Lima (2006) and Bodnar et al. (2007) by presenting a thermodynamic description of the earlier semi-quantitative models. The model presented here is consistent with geological, geochemical and geophysical data and results in a more complete understanding of bradyseism at CF. A quantitative model for subsidence and uplift is presented based on the linkage between bradyseism and magma body cooling and concomitant crystallization and fluid phase exsolution and the coupling of long timescale magma crystallization and volatile exsolution from melt and expulsion from magma to shorter timescale hydrothermal system behaviour. Hurwitz et al. (2007a,b) have recently shown by numerical simulation of hydrothermal flow that small changes in the permeability field including its anisotropy can lead to large differences in the rate, magnitude and geometry of GSD (i.e., bradyseism) independent of the underlying magmatic system. Here we focus upon the thermodynamics of fluid expulsion from magma as a result of crystallization, referred to as 'second boiling' and fluid decompression by isenthalpic expansion, mineral precipitation and concomitant permeability changes in the shallow crust

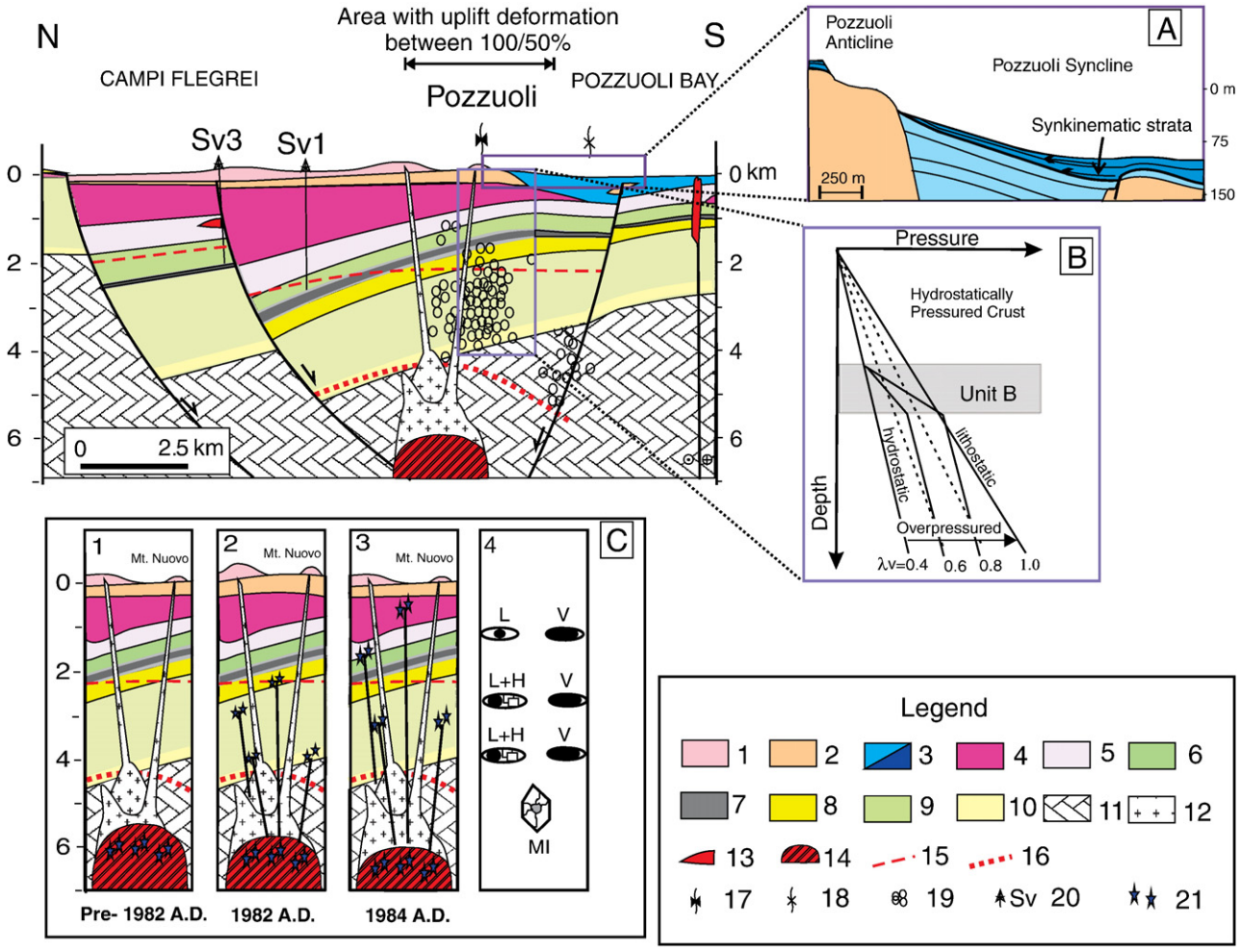

Fig. 3. Geologic section across Campi Flegrei–Pozzuoli Bay (as dashed line in Fig. 1). 1. Holocene volcanics; 2. Neapolitan Yellow Tuff; 3. Main sediments post 39 ka; 4. Campania Ignimbrite and pre-CI tuffs; 5. Middle Pleistocene sandstones, siltstones and volcanics; 6. Middle Pleistocene marine sediments (sandstones and siltstones — unit C in text); 7. Fine grained Middle Pleistocene marine sediments (claystones and siltstones — Unit B in text); 8. Middle Pleistocene deep water debris flows; 9. Lower Pleistocene marine sediments; 10. Continental deposits and conglomerates; 11. Meso-Cenozoic substrate; 12. Crystallized magma; 13. Volcanic bodies; 14. Magma body; 15. Thermometamorphic boundary; 16. Impermeable zone surrounding the crystallizing magma body. 17. Pozzuoli Anticline; 18. Pozzuoli Bay Syncline; 19. 1983–84 earthquake hypocenters; 20. Deep geothermal wells; 21. Magmatic fluids. Inset A: North–South cross section showing Pozzuoli Anticline–Syncline and the synkinematic strata. Inset B: Pressure–depth relationships across the relatively impermeable layer (Unit B) shown in terms of the pore-fluid factor, λ_v, with hydrostatic gradients preserved in the relatively high permeability rock above and below the claystones and siltstones of Unit B. Maximum overpressure is governed by the local compressional stress regime, the prevailing level of differential stress, and the absence of inherited brittle structures. Inset C: Schematic interpretation of subsurface magmatic–hydrothermal activity at Campi Flegrei (1) Following the 1538 eruption, the magma body became a closed system, and magmatic volatiles accumulated below impermeable crystallized carapace. (2) In 1982, the carapace confining the magmatic system fractured, allowing magmatic fluids to enter the overlying rocks beneath the low-permeability caprock (Unit B), causing vertical ground deformation. (3) Ground deformation that began in 1982 ended and deflation began when fractures penetrated the low-permeability cap rock, allowing the deep fluids to migrate into the shallow hydrostatic aquifers and flow toward the surface. (4) Systematic variation in the types of fluid and melt inclusions that occur at different depth (abbreviations: L = Liquid-rich inclusion; V = Vapour-rich inclusion; L + H = Halite-bearing fluid inclusion; MI = Melt inclusion).

beneath CF. The *in situ* structure of permeability resulting from the sedimentary structure of the crust is incorporated into the model presented. An improved understanding of bradyseism at CF leads to more realistic evaluations of volcanic risk and eventually, the development of more informed response plans.

2. Campi Flegrei bradyseism, models of inflation and deflation and relationship to volcanism

For many hundreds of years changes in sea level quantified by boreholes left by marine molluscs in the columns of the Serapis Temple have fascinated researchers (Breislak, 1792; Forbes, 1829; Niccolini, 1839, 1845; Babbage, 1847; Lyell, 1872; Gunther, 1903). Dvorak and Mastrolorenzo (1991) updated the work of Parascandola (1947) on the boreholes and reconstructed the history of CF vertical movements. More recently, Morhange et al. (2006) documented three relative sea level high stands using radiocarbon dating of biological materials at Serapis; the third one occurred in 1538 A.D., when uplift of about 7 m occurred immediately before the Monte Nuovo eruption (Fig. 2). Within the past 2000 years, there have been many phases of GSD not associated with volcanic eruptions. Although the emplacement of magma at shallow depth generally does lead to GSD, it does not follow that active bradyseism implies magma has been recently emplaced or that an eruption is imminent. In fact, the record at CF suggests just the opposite: only once (1538 AD) has bradyseism been shown to have been associated with volcanism. This is true not only at CF but also in other regions characterized by significant bradyseism such as at Yellowstone (Pierce et al., 2002; Lowenstern and Hurwitz, 2007) and the Long Valley caldera (Hill et al., 2002; Foulger et al., 2003). Although bradyseism is restricted to volcanic regions, bradyseism and volcanic eruptions imperfectly correlate.

Various models have been proposed to explain GSD at CF. The mechanical model — mostly popular in the 1970s — attributes unrest episodes to the intrusion of new magma at shallow depth (Corrado

et al., 1976; Berrino et al., 1984; Bonafede et al., 1986; Bianchi et al., 1987). Recently, Bellucci et al. (2006), in the light of new calculation of uplift and subsidence rates at CF from Roman times, proposed again this model interpreting the behaviour in terms of the intermittent ascent of magma between a reservoir of ~10^2–10^3 km^3 at depths of 8–15 km or greater, to a much smaller, shallower system at depths of about 3–4 km. An alternative model explains the unrest as being mainly the result of heating and expansion of fluids (Oliveri del Castillo and Quagliariello, 1969; Casertano et al., 1976; Todesco et al., 2003, 2004; Battaglia et al., 2006; Troise et al., 2007; Caliro et al., 2007). Other researchers explain the unrest mainly as being the result of fluid-dynamic processes in the shallow geothermal system (Bonafede, 1990, 1991; De Natale et al., 1991; De Natale et al., 2001; Trasatti et al., 2005). Still others (Cortini et al., 1991; Cortini and Barton, 1993; Cubellis et al., 2002) proposed more generalized non-linear dynamical models based on chaos theory. De Natale et al. (2001) and De Vivo and Lima (2006) summarize the strengths and weaknesses of the various models.

Seismicity at CF occurs only during unrest episodes (Corrado et al., 1976; De Natale et al., 1995). During 1982–84 more than 16,000 earthquakes occurred, ranging from 0.4 to 4.0 in magnitude (Aster et al., 1992). De Natale et al. (1995) postulated the presence of faults associated with an inner caldera collapse structure based on seismological studies. Gravity studies (Berrino et al., 1984; AGIP, 1987; Berrino et al., 1992; Berrino and Gasparini, 1995) show a minimum in the Bouguer anomaly located in the CF. Other seismic studies (Aster and Meyer, 1988; Ferrucci et al., 1992) define a shallow low-velocity anomaly interpreted as a magma body.

A selection of the seismic events recorded at CF, as a consequence of the last bradyseism episode in 1983–84, has been analysed by Guidarelli et al. (2002) to obtain Rayleigh wave group velocities and tomographic maps for the CF area. The obtained group velocity data of short period have been merged with the cellular dispersion data for the whole Neapolitan volcanic region (Panza et al., 2004, 2007). In this way, structural models for CF up to depths of about 30 km have been retrieved from the non-linear inversion of the dispersion curves with hedgehog method (Guidarelli et al., 2006 and references therein). A low shear wave velocity layer has been found at about 10 km depth consistent with that found below Mt. Vesuvius at 8 km depth with a similar inversion procedure applied to local earthquakes.

Recently, some Mt. Vesuvius events recorded in 1999–2000 at INGV-OV stations in the Campi Flegrei volcanic area have been processed to obtain group velocities of Rayleigh-wave fundamental mode (Nunziata, submitted for publication). Regional group and phase velocity data, recently reviewed and improved, have been considered as well, at the inversion stage. Average shear wave velocity (V_S) models for the uppermost 73 km of the lithosphere below the Neapolitan area, midway between CF and Mt. Vesuvius volcanic areas, have been obtained by means of the hedgehog nonlinear inversion method. A main feature of the obtained structural models is represented by low V_S velocities at around 9 km depth. This low-velocity layer has been found also below CF at the same depth and below Mt. Vesuvius at 6 km depth, and can be associated with the presence of quite diffuse partial melting.

Ground deformation and seismicity are associated with intense fumarolic and hydrothermal activity, concentrated in the crater of Solfatara, where CO_2 fluxes are particularly intense during uplift, reflecting magmatic degassing (Chiodini et al., 2003). The same fumarolic fluids, based on their stable isotopes, are interpreted as magmatic fluids variably contaminated by connate and meteoric components (Allard et al., 1991; Todesco and Scarsi, 1999; Panichi and Volpi, 1999).

More recently, models based on the interaction of magmatic fluids with hydrothermal systems dominated by non-magmatic fluids have been proposed by Gaeta et al. (2003), Todesco et al. (2003, 2004), Todesco and Berrino (2005), Battaglia et al. (2006), Troise et al. (2007) and Caliro et al. (2007). Todesco et al. (2003, 2004) and Todesco and Berrino (2005) associate the GSD as being triggered by pressure variations in the hydrothermal system. In particular, Todesco et al. (2003) indicate that an increase in the permeability at shallow depth may have an important influence on the system conditions and fluid discharge. Battaglia et al. (2006) indicate that the migration of fluids to and from the caldera hydrothermal system is the cause of ground deformation and consequent unrest. The same authors infer that the "intrusion of magma takes place at the beginning of each period of unrest" and suggest that uplift may be used to forecast eruptions at CF. According to Caliro et al. (2007) the magmatic component fraction (X_{CO_2}/X_{H_2O}) in fumaroles increases (up to ~0.5) during each seismic and ground uplift crisis, suggesting that bradyseismic crises are triggered by periodic injections of CO_2-rich magmatic fluids near the base of the hydrothermal system. The decrease of the X_{CO_2}/X_{H_2O} ratio corresponds to a period of low flux of the magmatic component and of depressurization of the hydrothermal plume, in agreement with GSD which accompanies periods of CO_2/H_2O decrease. Troise et al. (2007) associate the uplift with input of magmatic fluids from a shallow magma chamber, based on continuous GPS data on the ratio of maximum horizontal to vertical displacement. According to these authors "the small ratio between horizontal and vertical displacements during the small uplift episodes is indicative of overpressure in the deeper source of fluids of magmatic origin, whereas a large uplift episode could occur when the initial pulse of overpressure, after significantly fracturing the upper rocks, migrates into the shallower aquifers". In particular, in the models of Battaglia et al. (2006) and Troise et al. (2007) magma plays an active role in uplift and possibly eruption. Finally, in the model of Bodnar et al. (2007) fluid expelled by crystallization of pre-existing magma supplies the fluids involved in bradyseism, but is not the intrusion of new magma to play an active role in uplift episodes. Bodnar et al. (2007) predict that uplift between 1982 and 1984 is associated with crystallization of ~0.83 km^3 of H_2O-saturated magma at ~6 km depth. The latter depth is in good agreement with the recent findings of Esposito et al. (2009a,b). During crystallization, ~6.2×10^{10} kg of H_2O and 7.5×10^8 kg of CO_2 exsolves from the magma and generates ~7×10^{15} J of mechanical ($P\Delta V$) energy to drive the observed uplift at CF. Near the approximate depth of the magma-country rock interface indicated by Bodnar et al. (2007), recent results of seismic tomography (Zollo et al., 2008) indicate a magma sill at ~7.5 km depth. The latter results amplify the concept that shallow level magma intrusion at CF is not the cause of bradyseism and uplift. According to Bodnar et al. (2007), the solid–melt boundary of the mush zone of the crystallizing magma body migrates downward and fresh magma injection is not a pre-requisite for bradyseism (as illustrated schematically in Fig. 3C). This aspect of the Bodnar model is a major difference with previous models. The subsurface magmatic–hydrothermal activity at CF for the period pre-1982 and 1984 A.D. is schematized in Fig. 3C (1–3). Evidence for connectivity between the deep and shallow systems is provided by CO_2/H_2O ratios of fumarolic fluids at CF (Fig. 4), which increase during uplift and reach a maximum shortly after deflation begins (i.e., after the low-permeability cap rock is breached).

3. Geologic framework

In the Campania margin the stratigraphic architecture, depositional environments and rate of subsidence and sediment supply are controlled by normal fault activity (Milia and Torrente, 1999). The Campania margin is characterized by extensional structures that affected the Apennine fold-thrust belt and formed half grabens during the Pleistocene (Fig. 1). The CF–Bay of Naples area corresponds to a half-graben basin, bounded by NE-trending normal faults (Milia et al., 2003). The tilting of the Bay of Naples fault block is responsible for the lateral change in the physiography from shelf to slope to the

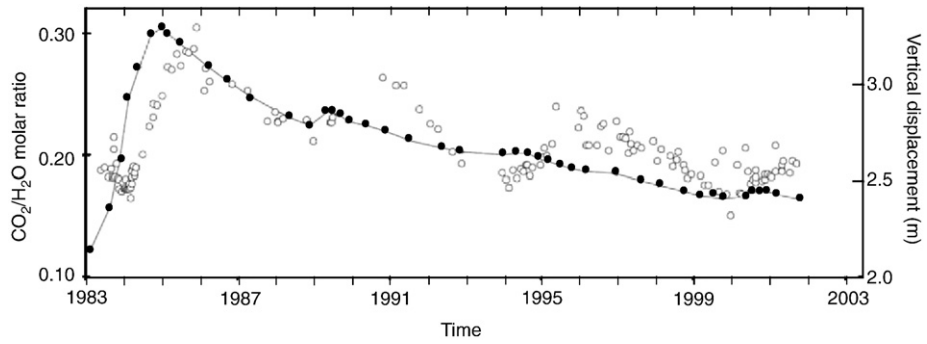

Fig. 4. CO_2/H_2O recorded at La Solfatara fumarole, in the last 20 years, plotted versus time and also compared with vertical displacement measured at Pozzuoli since 1983 (after Chiodini et al., 2003).

deep basin. The block tilting is associated with the formation of a tectonically enhanced unconformity on the crest of the block in the shelf area, and deposition of coeval thick debris flows in the deep basin.

The correlation between the seismic units recognized in the Bay of Naples with outcrops and well logs, and with dated successions and dated fault activity, enables reconstruction of the stratigraphic succession along the Campania margin (Milia and Torrente, 1999; Milia et al., 2003). The basement corresponds to the Mesozoic-Cenozoic carbonate succession forming the Apennine thrust belt. Terrigenous conglomerates overlie carbonates. A marine succession of siltstones and calcarenites of Lower Pleistocene age lies above the conglomerates. Following the CF–Naples Bay half graben formation, a tectonically enhanced unconformity formed on the shelf area and relatively thick debris flows were deposited in the basins. A Middle Pleistocene stratigraphic succession characterized by a transgressive–regressive cycle rests above the debris flow unit. The transgressive succession (Unit B), deposited between 0.7 and 0.4 Ma, corresponds to claystone–siltstone composed of fine-grained pelagic and hemipelagic sediment, characteristic of deepwater environments associated with transgressions and high stands of sea level. The regressive succession (Unit C) is mainly composed of coarser grained clastic sediments interlayered within the hemipelagic succession. In the upper part of the C unit, numerous ignimbrites and volcanic units are deposited (Milia and Torrente, 2007). Offshore CF, numerous monogenetic volcanoes and volcanoclastic deposits fill the marine basin (Milia et al., 2006) The CF stratigraphic sequence (Fig. 3) is based on data from the 3000 m deep San Vito and Mofete geothermal wells (Fig. 1) (De Vivo et al., 1989, and unpublished data). The uppermost 2000 m is composed of recent volcanoclastic products with minor trachytic volcanics. Of specific relevance to the current study is the presence of a low permeability cap rock (unit B) at a depth of about 2–3 km (Fig. 3). In the San Vito boreholes (Fig. 1), a systematic increase in metamorphic grade with depth is observed below about 2 km. The thermal profile associated with this metamorphic aureole suggests that magma was present at a shallower depth (4–5 km) in the past compared to today ($\geq$6 km).

The lithological characteristics of the regional stratigraphic succession depicted in Fig. 3 define a permeability structure that is critical to the bradyseism mechanism proposed in this study. In particular, there are two important aspects. The first is the anisotropy in permeability defined by the sedimentary layering such that the component of the permeability parallel to bedding exceeds the component orthogonal to layering (e.g., McKibben and Tyvand, 1982; Rosenberg et al., 1993). The second aspect is the vertical variation in the magnitude of the permeability (Bredeholft and Hanshaw, 1968; Neuzil, 1995). The upward movement of fluid released by magma degassing is impeded by low-permeability layers. Based on stratigraphic relations, from the surface downward into the crystallized rind of the magma body the permeability oscillates from high (coarse clastics and volcanoclastics) to low (transgressive siltstones and claystones) to high (debris flows) to low (marine calcarenites and siltstones) to high (fluvial conglomerates) and finally to low (carbonates, thermometamorphic and plutonic rocks) values. The structure and magnitude of the permeability field is an important component of our model of bradyseism at CF.

The Campania Margin is a tectonically active area. In particular during the 700 ka and 400 ka time interval a NW–SE extensional tectonics was responsible for the formation of deep basins, one of them the CF (Milia and Torrente, 1999). During the late-Quaternary uplifting areas and E–W left lateral strike slip faults were documented along the margin contemporaneous to the activity of normal faults. The faults and folds documented in the Campania Margin area are compatible with block rotation resulting from a trans-tensional shear zone, characterized by east-trending left lateral and NW–trending extensional movements, active along the eastern Tyrrhenian Sea margin during the Late Quaternary (Milia and Torrente, 2003). The structural framework of the studied area is characterized by high angle faults that affect the boundary of the CF area onshore and offshore. In the Bay of Pozzuoli, corresponding to the southern part of the CF, active folding is occurring (Milia et al., 2000; Milia and Torrente, 2000). The main fold is an anticline culminating near the city of Pozzuoli and a syncline located in the Bay of Pozzuoli (Fig. 3, inset A). Structural and stratigraphic analyses yield quantitative data on the timing of fold inception, kinematics, and the amount and rates of uplift. The rate of fold uplift ranges from 1 to 20 mm/yr. The structures show limb rotation kinematics and decreasing uplift rates. The uplift rates and geometry of the Pozzuoli Bay folds suggest that they are of tectonic origin, a product of detachment folding.

At CF the maximum uplift associated with bradyseism corresponds to the anticline culmination (near Pozzuoli) where a compressional tectonic regime is active; the uplift decreases rapidly toward the CF boundary where the main high angle faults occur. Earthquakes associated with bradyseism are located close to Pozzuoli and in the middle of the Bay near the focus of the tectonic folding. The maximum depth of the earthquakes is located at the stratigraphic boundary between the carbonates of the Mesozoic–Cenozoic succession and the overlying stratified clastic succession of Pleistocene age.

According to Sibson (2003), the maximum overpressure is governed by the tectonic regime, the prevailing level of differential stress, and the presence or absence of inherited brittle structures. Indeed, because of the contrasting slopes of the failure curves, it is generally easier to sustain fluid overpressure in a compressional regime; conversely, sub-vertical extension fractures and steeply dipping normal faults promote high vertical permeability, contrasting with sub-horizontal extension fractures and low dipping faults in compressional regimes. The mechanical dependence of different brittle-failure modes on both stress state and fluid pressure is also a critical factor. Super-lithostatic fluid pressures ($\lambda_v > 1.0$) are only likely to be attained in compressional regimes under low levels of differential stress in the

absence of a fault favourably oriented for slip reactivation (Fig. 3, inset B). At the boundary of the CF region the presence of low-cohesion faults oriented for reactivation in the prevailing stress field inhibit hydraulic extension fracturing in intact rock, providing a lower bound to maximum sustainable overpressure for a given differential stress.

4. Campi Flegrei magmatic–hydrothermal conceptual model

The authors interpret ground movement at CF to be the result of magmatic–hydrothermal processes (without invoking the input of new magma from below) driven by crystallization of hydrous magma at depth with concomitant exsolution of fluid from melt and the eventual expulsion of lithostatically pressured fluid into overlying country rock. The petrologic basis for generation of magmatic fluids by 'second boiling' is documented elsewhere in considerable detail for CF magmas (Fowler et al., 2007). The deep fluid environment at CF is similar to that documented in magmatic–hydrothermal ore deposit systems associated with porphyry copper deposits (Bodnar and Beane, 1980; Beane and Titley, 1981; Audétat and Pettke, 1993; Bodnar, 1995; Beane and Bodnar, 1995; Roedder and Bodnar, 1997; Sasada, 2000).

Porphyry copper deposits are magmatic–hydrothermal ore deposits that form in the continental crust overlying subduction zones at convergent plate margins. For purposes of this discussion, we assume that melt and fluid evolution that has been documented in porphyry copper deposits applies, in a general sense, to the crystallization of intermediate to silicic volatile-bearing magmas. When hydrous magmas in the upper crust cool and crystallize, a volatile phase is exsolved from the melt. The fluid is usually a low salinity, H_2O-rich fluid that contains various amounts of CO_2, H_2S or SO_2, and ore metals such as Cu, Au, Mo, Pb, Zn and Ag (Bodnar, 1995; Roedder and Bodnar, 1997) as well as small amounts of non-metal and metal soluble major elements such as K, Rb, Cs, Ba, Pb and Sr (Spera et al., 2007).

During initial crystallization of the under-saturated melt, the volatile content of the melt increases as anhydrous phases precipitate. Eventually, the melt becomes saturated in volatiles (usually CO_2 or H_2O) and the pressure in the magma body increases as the fluids are trapped beneath the impermeable igneous rock rind surrounding the magma. The magmatic volatiles that exsolve from the magma at variable depths between 4 and 10 km are usually low density single-phase fluids or, as is the case at CF and some other shallow systems (Cline and Bodnar, 1994), high salinity brine and vapour may exsolve directly from the magma (Fig. 5A). Owing to its greater density and viscosity, the high salinity liquid usually "ponds" in the deeper portions of the system, while the lower salinity, low-viscosity vapour phase migrates to shallower levels of the system. When the overlying impermeable rocks fracture, the low salinity gas moves towards the surface and interacts and mixes with meteoric water (or seawater) present in fractures and pores at shallow depths (Fig. 5C).

The variation in fluid properties with depth in the porphyry copper environment results in a systematic variation in the types of fluid and melt inclusions that occur with depth. In the deepest part of the system, crystals + silicate melt + magmatic fluid coexist and phenocrysts containing coexisting silicate melt inclusions and fluid inclusions are common and these same types of inclusions are found in crustal xenoliths from CF and surrounding areas. After the impermeable rock surrounding the magma body fractures, magmatic gas escapes and moves into overlying rocks where phase separation occurs to produce high salinity brines coexisting with low salinity vapour. Fluid inclusions that trap the high salinity liquid usually contain a halite crystal at room temperature, whereas those inclusions that trap the vapour phase are vapour-rich at room temperature (Fig. 3C4). In the shallowest parts of the magmatic–hydrothermal system, magmatic fluids mix with cooler and lower salinity meteoric or seawater to produce a low salinity boiling assemblage. Fluid inclusions that trap the liquid in this environment are low salinity liquid-rich, whereas those that trap the vapour are vapour-rich at room temperature (Fig. 3C4). So, as the system evolves, melt and fluid inclusions with distinct properties are trapped in phenocrysts and veins in these deposits (Bodnar, 1995; Bodnar and Student, 2006), and similar melt and fluid inclusions are observed in samples from CF (De Vivo et al., 1989; De Vivo et al., 1995, 2005, 2006).

Here we describe those observations at CF that are consistent with the crystallization of a volatile-bearing magma at depth (~6 km), and release of magmatic fluids into a deep lithostatically-pressured aquifer separated from a more shallow hydrostatic aquifer by a low-permeability region (~2.5–3.0 km depth) (Fig. 5). In a later section we describe a thermodynamic–transport model in which bradyseism is driven by the transient connection between the deeper lithostatic reservoir and an overlying more permeable hydrostatic one. In our model there are two timescales; one is the 10^3–10^4 yr timescale associated with magma solidification (and associated magmatic fluid generation). The second shorter timescale (1–10 yr) is intrinsically episodic in nature and associated with transient fracture propagation events that connect the lower lithostatic reservoir with the upper hydrostatic one (Figs. 3 and 5) until connectivity is dampened by mineral precipitation (e.g., deposition of silica) accompanying irreversible fluid decompression.

4.1. Energy and volume changes associated with volatile exsolution and boiling

When H_2O is dissolved in a silicate melt the partial molar volume of H_2O component dissolved in the melt represents its volume in the melt phase. In contrast, when the melt becomes saturated and exsolves a fluid phase, the volume of the magmatic gas is approximated by the molar volume of H_2O at the temperature and pressure of interest. The partial molar volume of H_2O in the melt varies relatively little with pressure and temperature (Lange and Carmichael, 1990; Lange, 1994) and lies in the range 13–20 cm^3/mol; however, the molar volume of supercritical H_2O varies over a wide range as a function of pressure at magmatic temperatures and becomes very large at low pressure (Burnham et al., 1969). As a result, when a hydrous melt becomes saturated in H_2O and exsolves a magmatic H_2O phase, the volume of the system (crystals + melt + fluid) increases significantly at constant pressure (Burnham, 1972, 1985). At pressures of 100–200 MPa, the system volume change can be 50% or greater, and even at 0.6 GPa (roughly 20 km depth) the volume of the system (crystals + melt + H_2O) will increase by about 10%. If the volume of the system is unable to expand to accommodate the volume increase (as in the case of magma that is surrounded by impermeable and rigid crystallization products), pressure increases. In an isochoric process, large amounts of mechanical energy are stored in the magma chamber (Fig. 6). It is this energy that leads eventually to fracturing and uplift of the overlying impermeable rocks, allowing the magmatic aqueous phase and, in some cases, magma, to escape into the overlying rocks.

In a similar way, when H_2O moves across the low-permeability cap rock layer, the pressure gradient changes from lithostatic to hydrostatic. As a rule of thumb, the lithostatic gradient is about 30 MPa/km, and the hydrostatic gradient is about 10 MPa/km. Thus, as the fluid moves from the lithostatic to hydrostatic domain and flows upwards along the hydrostatic gradient the fluid volume will tend to increase rapidly. There is also an abrupt decrease in the pressure itself that is associated with Joule–Thompson expansion and mineralization. This volume increase of fluid contributes to GSD at CF.

4.2. Comparison to other magmatic–hydrothermal systems

The model to explain ground deformation at CF is in many respects similar to the one proposed to explain deformation in the Long Valley caldera, California (Hill et al., 2002) and Yellowstone National Park (Fournier, 1989).

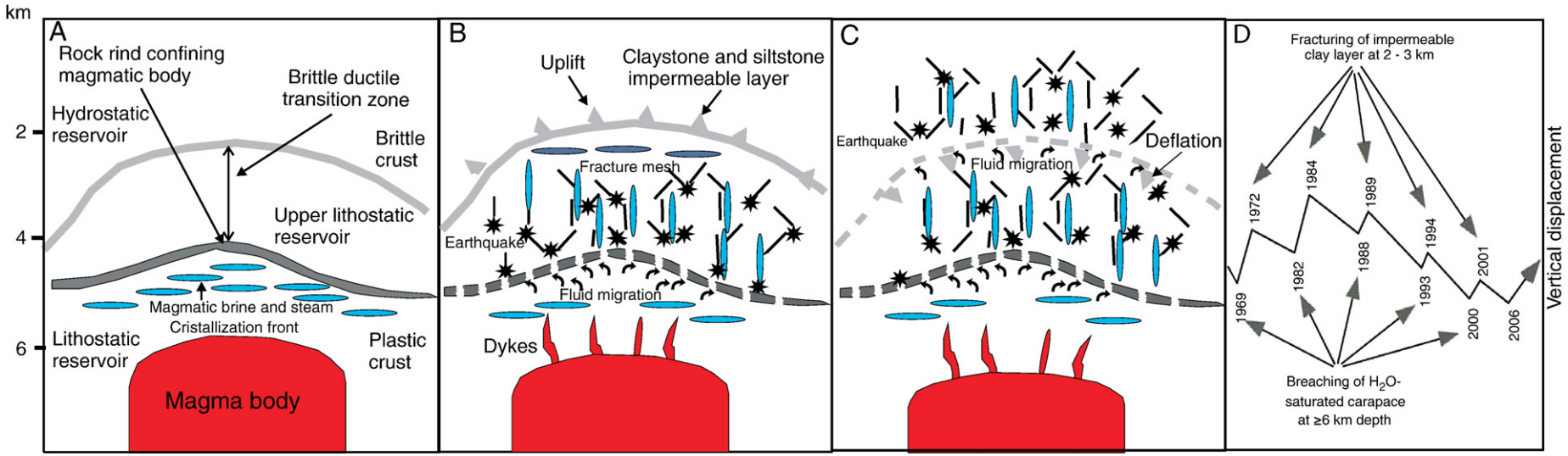

Fig. 5. Schematic pattern to show the relationships between magma, fluids and crustal deformation at CF. A: Sealed magmatic–hydrothermal system showing the plastic and brittle domains separated by an intermediate lithostatic–hydrostatic reservoir. B) The impermeable carapace confining the magmatic system allows magmatic fluids to enter the overlying rocks (transition ductile–brittle domain) beneath the low-permeability cap rock (unit B), causing ground uplift. C: Ground uplift ends and deflation begin when fractures penetrate the surficial low-permeability cap rock, allowing the fluids to migrate into the shallow aquifers (hydrostatic domain) and flow toward the surface. D: Schematic representation of vertical ground displacement at Campi Flegrei. Note that both vertical displacement and time are schematic and only indicate the direction of ground movement at different times.

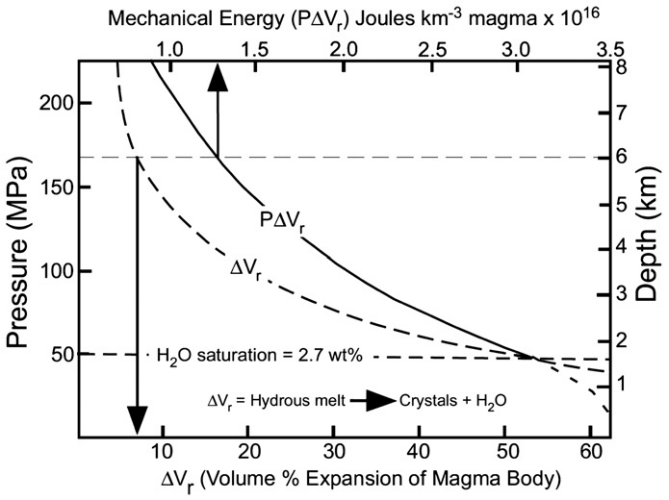

Fig. 6. Volume change (ΔV_r) and mechanical energy ($P\Delta V_r$) associated with crystallization of an H_2O-saturated melt. The calculated values assume a closed system (modified after Burnham, 1972, 1985).

At Long Valley a seismogenic brittle crust is separated from the underlying plastic crust and an embedded magma body by a transition zone. At CF bradyseism is triggered initially by breaching of the rock rind confining the magmatic system (brittle–ductile boundary), corresponding to the lower limit of the earthquake hypocenters (4 km), allowing magmatic fluids to enter the overlying rocks beneath the low-permeability cap rock (~2.5–3.0 km) and causing vertical ground deformation (Fig. 5A). Fracturing of the crystallized rind and the concomitant pressure drop resulted in a "pressure quench" of additional magma leading to the release of additional CO_2 from the magma. Accordingly, evidence for connectivity between the deep and shallow systems is provided by CO_2/H_2O ratios of fumarolic fluids at CF (Fig. 4), which increase during uplift and reach a maximum shortly after deflation begins (i.e., after the low-permeability caprock is breached).

Uplift ends and deflation begins when fractures penetrate the low-permeability cap rock (Fig. 5B), allowing the deep magmatic fluids to migrate into the shallow aquifers and flow toward the surface. This process may culminate in a steam blast, if water at shallow depths is heated to its flash point. A magmatic eruption may follow if the reduced confining pressure on the magma leads to a runaway process of bubble formation, ascent and growth (as was the case for the Monte Nuovo eruption at CF). A hydraulic surge can be triggered by the deformation induced by the active tectonics that characterize the CF area, disrupting the transition seal and allowing magmatic geopressured fluids to invade the country rock.

At CF, with the exception of the Monte Nuovo eruption, magma has not reached the surface in the last 3700 years. Rather, during fracturing of wall rock surrounding the magma body, magma travelled only into the overlying rocks to produce dikes and sills, releasing magmatic fluids into the deep aquifer. In the case of the Monte Nuovo eruption in 1538 A.D. a propagating melt-filled fracture penetrated the brittle–ductile transition zone and allowed magma to enter the shallow aquifer. The Monte Nuovo eruption began as a hydrothermal eruption that later evolved into a hydromagmatic eruption (Rosi and Sbrana, 1987). An eruption occurred because the overpressure generated by the magmatic–hydrothermal fluid was acting on rocks at a relatively shallow depth (≤500 m) above a low-permeability cap rock.

At Yellowstone National Park, Fournier (1989) and Dzurisin et al. (1990) propose a model whereby magmatic fluids liberated from crystallizing siliceous magma at a depth of 4–5 km ponds in a region where pore-fluid pressures are lithostatic. Accumulation of magmatic fluids at lithostatic pressure and episodic injection of a portion of this fluid into an overlying hydrostatically pressured system would account for the observed inflation and deflation of the caldera. According to Fournier (1989), episodic rupturing of self-sealed rocks separating regions of lithostatic and hydrostatic pore-fluid pressures could account for the seismic swarms occurring within the Yellowstone caldera. Hurwitz et al. (2007a,b) and Lowenstern and Hurwitz (2007) state that at Yellowstone intrusion of basaltic magma occurs in the lower-mid crust sustaining the overlying high-silica magma reservoir and flooding the hydrothermal system with magmatic volatiles. According to the latter authors, a number of issues remain unclear, however. In particular: What is the mechanism behind variation of the surface fluid flux at daily to millennial timescales? Does the current fluid and gas flow result from a temporarily increased rate of hydrothermal discharge reflecting shallow hydrothermal processes or an associated with deep intrusions? Possibly, increased hydrothermal flow is cooling the underlying magma, and hence decreasing the long-term volcanic hazard. That is, has Yellowstone been dormant for a long time because the magmatic– hydrothermal system is efficiently releasing heat and volatiles, precluding build up of magmatic pressure?

5. Three phase thermodynamic model for bradyseism

To test the magmatic–hydrothermal model outlined above, we have developed a simple analytical three-phase model that captures the essential thermodynamics of finite volume magma bodies undergoing simultaneous solidification and fluid phase evolution. Tait et al. (1989) presented a quantitative model of overpressure resulting from fractional crystallization and supersaturation of volatiles in a shallow magma chamber and the consequent increase in volume. Studies by Huppert and Woods (2002) and Woods and Huppert (2003) also provide a quantitative model of magma overpressure due to volatile exsolution. These models use a linear relationship between fraction of melt crystallized and temperature. However, realistic phase equilibria calculations using the MELTS model (Ghiorso and Sack, 1995) show that a logistic form of the melt fraction *versus* temperature relationship is more realistic. Such a form has been adopted here. Magma, of mass M_o, is injected into the shallow crust at some mean pressure p_o, equal to the local lithostatic pressure. Heat is lost from the magma and flows to cooler country rock. The crystallization of magma and concomitant exsolution of a magmatic fluid leads to a pressure increase if the crystallization takes place at constant volume (isochoric process) or to a volume increase (uplift) or volume decrease (subsidence) if crystallization is isobaric. In the latter case, the isobaric crystallization can occur in one of two ways. The system can be open, meaning that fluid is expelled from magma upon exsolution from melt or closed, meaning that exsolved fluid remains within the magma as a separate fluid phase (i.e., fluid bubbles are present in the magma). The fluid in this simple model is treated as pure H_2O although other volatiles (e.g., CO_2, SO_2, etc.) could be incorporated. Because the mass ratio of $H_2O/CO_2 \gg 1$, H_2O is a reasonable approximation to the properties of multicomponent geofluids at the level of a simple analytical model (Spera et al., 2007). The initial state of the system is taken as melt just volatile saturated (trace of H_2O bubbles) at its liquidus temperature $T_\diagup$ (trace of suspended solids). The mass fractions of melt, solid and fluid are denoted by $f_m = M_m/M_o$, $f_s = M_s/M_o$ and $f_f = M_f/M_o$. The initial condition on mass fractions are $f_m = 1$ and $f_s = f_f =$ trace. At the liquidus temperature, the initial volume of magma is V_o and the pressure is p_o. The dissolved H_2O content of the magma $w^m_{H_2O}$ is a function of pressure (the effects of temperature and melt composition are small compared to pressure) and the total mass fraction of water component in the system is Z^o_w. The model is executed by removing heat thereby triggering cooling and crystallization and concomitant exsolution of fluid and monitoring the fractions of melt, fluid and solid (f_m, f_f and f_s) as a function of

V and T or p and T, depending on whether heat is removed isobarically or isochorically. The fraction of melt, f_m is assumed to be a function of temperature. Magma pressure is calculated during the course of crystallization and fluid exsolution when the process is carried out isochorically (rigid wall rocks). In contrast, changes in magma volume are determined for isobaric crystallization. For isobaric open systems, fluids are removed and detumescence of the magma body is expected. For isobaric closed systems, exsolved fluids remain within the melt as a bubble suspension. In this case, the volume of magma expands and magma body expansion occurs. A temporal sequence of system behaviors can be related to bradyseism via the expulsion of fluids and associated changes in the volume of the system. One possible scenario is that crystallization begins under constant volume conditions (isochoric) and then, once the pressure of fluid exceeds wall rock strength of 10–100 MPa, failure occurs and further evolution takes place isobarically. In cases where wall rock has low permeability, exsolved fluid is not expelled from magma and hence inflation occurs. It is during this stage that uplift takes place. At later times or when host rock permeability permits, exsolved fluids are expelled from magma and become part of the overlying hydrothermal system. Subsidence takes place in this case because crystallization is associated with a 10–20% decrease in magma volume. A full presentation of the model is given in Appendix A.

Volume change can be converted to uplift or subsidence using the scaling $\Delta V/V_o \propto \Delta h/h_o$ where Δh is the uplift or subsidence associated with bradyseism. The magnitude of the volume changes associated with the phase transition is consistent with meters to tens of meters of elevation change of the magma body. The area on the Earth's surface affected is likely to be larger than simply the cross sectional area of the magma body and the magnitude of the uplift or subsidence will be concomitantly decreased. However, the scaling relation remains unchanged.

5.1. Magnitude of elevation changes: scale estimates

A limit can be obtained for the maximal uplift or subsidence based on the fractional change in system volume during complete isobaric crystallization (melt to solid plus fluid) under closed (uplift) or open (subsidence) conditions, respectively. When exsolved volatiles are not expelled from magma crystallizing isobarically (closed system), the fractional volume change from liquidus to solidus is

$$\frac{\Delta V}{V_o} = \frac{\rho_m^o}{\rho_s^o}\frac{(1-Z_w^o)}{(1+\alpha_s\Delta T)} + \frac{\rho_m^o \Re T_s}{p_o M_w} Z_w^o - 1 \quad (1)$$

where $\Re$ is the ideal gas constant, T_s is the solidus temperature (~1000 K), Z_w^o is the mass fraction of H_2O in the system (~0.04), p_o is the initial pressure at the depth of the magma body (6 km corresponds to 141 MPa), the density of melt, ρ_m^o and solid, ρ_s^o are 2200 kg/m^3 and 2700 kg/m^3, respectively, the expansivity of solid is 3×10^{-5}K^{-1}, and the solidus to liquidus temperature interval is 400 K. A scale estimate for the maximum fractional change in volume accompanying crystallization of a hydrous melt for these parameters is $\frac{\Delta V}{V_o} = +0.2$. All other factors remaining the same, if the depth to the magma body is 3 km instead of 6 km, then $\frac{\Delta V}{V_o} = +0.36$ (compare with volume expansion shown on Fig. 6). The latter is greater than the former because the density of fluid is inversely proportional to the pressure and more than compensates for the smaller solubility of water in melt at lower pressure (shallower depth). For isobaric open system behavior (fluid expelled from magma into country rock), the corresponding fractional volume change is $\frac{\Delta V}{V_o} = -0.22$ for a magma body at 6 km depth.

These estimates clearly show that volume changes associated with cooling, crystallization and volatile exsolution from magma can easily account for significant changes in topography characteristic of bradyseism. A better model is to allow for the non-ideality of H_2O as shown in Fig. 6; this has the effect of lowering the fractional volume changes during phase transition compared to the above estimates by about 20–30%.

Implied elevation changes can be estimated using the relation $\Delta h = \frac{1}{3} h_o \frac{\Delta V}{V_o}$. As an example, crystallization and fluid exsolution from 0.3 km^3 of melt in an equant magma body gives, for a scale elevation change in isobaric closed system evolution, $\Delta h = \frac{1}{3} V_o^{1/3}\left(\frac{\Delta V}{V_o}\right) =$ 40 m. This assumes that the area undergoing uplift is the same as the area of the top of the equant magma chamber; in fact the area undergoing uplift will be much larger than the area of the top of the equant magma chamber; hence this estimate is a maximum. This maximum estimate is based on retention of fluid exsolved from the melt upon crystallization and shows that significant topographic changes can be produced. When fluid is allowed to escape from the magma system, uplift is less. The increase in CO_2/H_2O ratio of fumarolic fluids indicates that fluids do indeed escape. If escape is very efficient, the volume change associated with magma crystallization is negative since solid (crystals), being denser, occupies less volume than melt and detumescence (collapse) rather than tumescence (uplift) occurs. The fractional volume change in this case (open system with respect to fluid) is $\frac{\Delta V}{V_o} = \frac{\rho_m^o}{\rho_s^o}\frac{(1-Z_w^o)}{(1+\alpha_s\Delta T)} - 1$ and is always less than zero (subsidence).

The applicable condition in a natural system depends on the ratio of the rate at which fluid is generated by second boiling relative to the rate that it is carried away by the overlying hydrothermal system (meteoric water plus magma volatiles). By coupling the heat loss to melt crystallization, the generation rate of fluid available for expulsion can be determined. With knowledge of the permeability of host rocks, the efficiency at which magmatic fluids are expelled into country rock can then be estimated. This also requires an estimate of the pressure gradient. One limit is for magmatic fluid at lithostatic or near lithostatic pressure to establish connectivity with fractured and permeable brittle crust in which hydrostatic or near-hydrostatic conditions exist.

5.2. Decompression of hydrothermal fluids: a mechanism for episodicity

An integral part of the bradyseism model is the episodic mechanical connection between a deeper geostatically pressured magmatic–hydrothermal reservoir (~4.5–6.0 km) with a shallower hydrostatic one (above 2.5–3.0 km). These two reservoirs are separated by a transition zone which episodically behaves as a ductile or brittle domain. This connectivity is established transiently by the propagation of cracks initiated by tectonic instability and hydrofracture related to brittle failure in the region separating the two, sometimes connected and sometimes distinct, systems. Transient high permeability pathways from the deeper to shallower reservoir allow for the transient decompression of aqueous fluids of meteoric and magmatic origins from high to lower pressure. Earthquake swarms during bradyseism is the manifestation of brittle failure to create cracks through which aqueous fluid travels during decompression (volumetric expansion of fluid). Fluid inclusions record portions of the complex geochemical history of these fluids (De Vivo et al., 1989, 1995, 2006). The temperature–pressure path followed by fluid can be approximated using a one-dimensional fluid dynamic model of vertical compressible flow of a single-phase fluid moving through rough cracks. The expressions for mass, momentum and energy conservation for compressible single-phase fluid of density $\rho=\rho(p, T, m_i)$ for flow in a vertical (z direction) crack of width w are written (Spera, 1981; see also Wallis, 1969)

$$\frac{du}{dz} = \frac{-\dot{M}}{\rho^2}\frac{d\rho}{dz} \quad (2)$$

$$\frac{dp}{dz} = -\dot{M}\frac{du}{dz} - \frac{2C_f\dot{M}^2}{w}\frac{1}{\rho} - \rho\vec{g} \quad (3)$$

$$\frac{dT}{dz} = \mu_{JT}\frac{dp}{dz} - \frac{u}{C_p}\frac{du}{dz} - \frac{4h(T-T_w)}{C_p\dot{M}w} - \frac{\vec{g}}{C_p} \quad (4)$$

$$\rho = \rho(p, T, m_i) \quad (5)$$

Eq. (5) is the equation of state of the hydrothermal fluid. Eqs (2)–(5) are valid for steady flow through a crack of width w. The Joule–Thompson coefficient, a purely thermodynamic parameter is defined $\mu_{JT} = (\alpha T - 1)/\rho C_p$ where α is the fluid isobaric expansivity, M^Y is the mass flux (kg m^{-2} s^{-1}) of fluid through a single crack of width w, u is the fluid velocity, C_f is the friction factor for fluid flow in the crack, h is the heat transfer coefficient for heat exchange between fluid and surrounding wall rock at ambient temperature, T_w and C_p is the specific isobaric heat capacity of fluid. For adiabatic ($h = 0$) flow and neglecting heats of reaction due to precipitation, hydrolysis and alteration reactions, combining Eqs. (2)–(4) leads to an expression for the temperature–depth trajectory of migrating fluid

$$\frac{dT}{dz} = -\mu_{JT}\frac{2C_f\dot{M}^2}{\rho w} - \frac{\alpha T\vec{g}}{C_p} \quad (6)$$

where the explicit dependence of the temperature change of the fluid on the Joule–Thompson coefficient and the irreversible part of the pressure drop via friction is noted. For frictionless flow, $C_f = 0$ and Eq. (6) reduces to the familiar expression for frictionless adiabatic (i.e., isentropic) flow. In contrast, applied to a situation where a sudden (irreversible) drop in pressure occurs such as between lithostatic and hydrostatically-pressured reservoirs, scale analysis of Eq. (6) for the temperature change (δT) associated with pressure drop δp due to adiabatic irreversible (throttling) decompression along a geopotential ($\delta z = 0$) gives

$$\delta T = \mu_{JT}\delta p. \quad (7)$$

Now, in decompression δp is negative so the sign of the change in temperature — that is, whether fluid heats up ($\delta T > 0$) or cools ($\delta T < 0$) upon expansion depends solely on the sign of the Joule–Thompson coefficient. The Joule–Thompson coefficient becomes increasingly negative (i.e., fluid heats up upon expansion) for expansions starting at high pressure, low temperature, high m_{NaCl} and high X_{CO_2} (Wood and Spera, 1984). If connectivity is established at a depth z_o of, say, 3 km where the pressure difference between the reservoirs (one lithostatic and one hydrostatic) is of order −60 MPa (i.e., $\delta p = -\Delta\rho g z_o$), then, based on a typical value of μ_{JT} of ~−0.2 K/MPa, fluid would experience a temperature *increase* of about +30 K upon irreversible decompression. In contrast, if fluid was to undergo this same decompression adiabatically and reversibly (i.e., isentropically) then the fluid would *cool* by ~+25 K, found by setting $C_f = 0$ in Eq. (6), using the usual relationship between lithostatic pressure and depth and appropriate thermodynamic properties.

Relevant to bradyseism is the possibility that throttling decompression could lead to a mechanical toggle such that connectivity between hydrostatic and lithostatic reservoirs is episodically turned on and off. The basis for this possibility can be explored by considering the effect of fluid temperature on silica solubility. That is, if connectivity is established and fluid expansion occurs, then the temperature increase associated with fluid decompression will lead to a decrease in the solubility of silica in the fluid. For example, using the solubility model of Walther and Helgeson (1977), the molality of aqueous silica decreases from $10^{-1.30}$ molal at 0.1 GPa and 600 °C to $10^{-2.1}$ molal at 0.04 GPa and 630 °C along the fluid isenthalp. Based on these solubility values, each kilogram of fluid undergoing decompression will precipitate about 3×10^{-3} kg of silica. Precipitation of silica will tend to seal cracks and hence aid in the reestablishment of isolated lithostatic and hydrostatic reservoirs, which could then, subsequently, reestablish connectivity following yet another phase of tectonic tumescence and fracture propagation.

5.3. Seismic energy and crack propagation

There have been many geophysical studies relating uplift and subsidence to observable geophysical and geochemical parameters of the 1982–1984 and other bradyseism events (Berrino et al., 1984; Martini et al., 1991; Vilardo et al., 1991; Zuppetta and Sava, 1991; De Natale et al., 1991; Dvorak and Gasparini, 1991; Yokoyama and Nazzaro, 2002; Chiodini et al., 2003; Yokoyama, 2006; Saccorotti et al., 2007). The bradyseism crisis during 1982–1984 was associated with a net uplift of ~1.8 m centered on Pozzuoli. The volume associated with the 1982–1984 bradyseism uplift approximated as a flat circular cone of radius 5 km and height 2 m was about 5×10^7 m^3. A magnitude (M) 3.4 earthquake on 15 May 1983 was followed by a 15-month period when more than 16,000 earthquakes with focal depths between 2 and 4 km were recorded. The largest earthquake was a M 4.2 event on 4 October 1983.

Waveform inversions have been performed for 14 selected earthquakes of 1984 seismicity in order to retrieve the seismic moment tensor components (Guidarelli et al., 2002). Focal mechanisms were found with the P and T axes oriented, in agreement with the stress field found in the area by other independent studies (De Natale et al., 1995). The moment tensor M_0 is commonly decomposed into the isotropic (V) part representing volume changes, the compensated linear vector dipole (CLVD) component that is related to lenticular crack activation accompanied by possible fluid motion, and double couple (DC) part due to dislocation movements. Guidarelli et al. (2002) showed that the reliable percentages of DC, CLVD, and V components reveal most of the events as being deviatoric and that the observed increments of V and CLVD components occur in correspondence with the increase of seismic rate. This may also be associated to an overpressure that is produced by heated shallow aquifers which are claimed to be a cause for ground deformation.

Here we test the hypothesis that the creation of fracture surface as implied by the propagation of fluid-filled hydrofractures is an important component of the energy budget associated with bradyseism, in particular the relationship between volume change and the total seismic moment and energy released. This analysis is offered in the spirit of a scale analysis and not a detailed seismological study. However, it does serve to test the hypothesis that inflation and GSD is related to the poroelastic effects of fluid migration in the shallow crust and associated hydrofracture.

We use the energy balance by Kostrov and Das (1988) for a single earthquake

$$E_s = -2S\gamma_{eff} + \frac{1}{2}\int_{\Sigma_1}(\sigma_{ij}^o - \sigma_{ij}^f)a_i^f n_j dS + \int_0^{t_m} dt \int_\Sigma \dot{\sigma}_{i,j} a_i n_j dS \quad (8)$$

to derive a scale expression involving fracture surface area and the radiated seismic energy given some nominal estimates of other parameters. In Eq. (8), E_s is the total energy transmitted by seismic waves through surface S_o surrounding the source, t_m is the earthquake duration, S is area of crack surface Σ_1, σ_{ij}, σ_{ij}^o and σ_{ij}^f represent stress tensors with subscript o and f for initial and final states and a_i^f and a_i represent displacements. We assume that hydrofracture is a mode I tensile deformation and that the stress driving fracture is fluid pressure slightly in excess of σ_3, the minimum principal stress taken to lie horizontally. The average shear wave velocity at Campi Flegrei is $V_s = 1.2$ km/s (Guidarelli et al., 2006). Assuming V_p/V_s of 1.85, the average V_p equals 2.2 km/s, E~8 GPa, the rigidity is μ~3 GPa and Poisson's ratio is ν=0.29. With the additional scale quantities $a = 10^{-2}$ m, $\gamma_{eff} = 0.5$–1 MJ/m^2, $\Delta\sigma = 1$–10 MPa and $E_s \sim 3\times10^9$ J, Eq. (8) indicates a typical fracture surface area of 10^4 m^2 (100 m by 100 m). Using the cumulative seismic energy radiated during the 1982–1984

bradyseismic crisis of 4×10^{13} J (De Natale et al., 1991) the cumulative fracture area for all crisis events is ~10^7–10^8 m^2. For a typical fracture area of 10^4 m^2, this implies creation of thousands of new hydrofractures during the bradyseism crisis. This calculation supports the notion that decompression of fluids via the propagation of fluid-filled cracks is an integral part of the bradyseism activity at CF.

Finally, we can relate the total seismic energy radiated during the bradyseismic crisis of 1982–1984 to the volume change and hence uplift. In this model, it is assumed that the earthquakes occurred in response to the injection of fluid into impermeable rock. The change in volume produces shear stresses that are released by earthquakes. McGarr (1976) has shown that in such a case the relationship between the cumulative sum of seismic moments ($\sum M_o$) and the total volume change ΔV is

$$\sum M_o = K\mu|\Delta V| \tag{9}$$

where K is a constant of order unity, μ is the rigidity modulus (~5 GPa at CF) and ΔV the volume change. If in Eq. (9) we consider the cumulative sum of seismic moments computed for the 18 strongest events, that is 18.7×10^{13} Nm (Guidarelli et al., 2002), a lowest bound of 5.7×10^4 m^3 can be estimated for the volume change. The seismic moment in turn is related to the seismic energy radiated by the earthquakes according to

$$M_o = \frac{2\mu\Delta E_{seismic}}{\Delta\sigma} \tag{10}$$

where $\Delta\sigma$ is the stress drop associated with a typical earthquake. Eqs. (9) and (10) can be combined to relate the total seismic energy radiated by earthquakes to the volume change ΔV. The relationship is

$$\Delta V = \frac{4\sum E_{sesmic}}{\Delta\sigma} \tag{11}$$

which gives a volume change of 5.3×10^7 m^3 for a mean stress drop of 3 MPa. This compares quite well to the observed volume of uplift of 5×10^7 m^3 based on geodetic measurements. This agreement supports the notion that bradyseism is related to the injection of fluids.

6. Summary

Based on magmatic–hydrothermal and thermodynamic models and considering the stratigraphy and structure of the CF area, we interpret the bradyseismic events in the CF volcanic region to be the consequence of a two-stage process. Fluid exsolution from melt followed by expulsion from magma during cooling and crystallization of residual magma generates magmatic fluid on a conduction timescale of 10^3–10^5 yr. This fluid remains geopressured (isobaric crystallization) or even super-geopressured (isochoric crystallization) until fracture propagation enables the expulsion of magmatic fluids. When hydrous melt becomes saturated in H_2O and exsolves a magmatic H_2O phase, the volume of the system increases significantly at constant pressure. When rock rind (brittle–ductile transition zone) around the magma chamber is breached, geopressured fluids escape into the overlying rocks, beneath low permeability strata (cap rock) and uplift occurs (Fig. 5). Ground deformation ends and deflation begins when fractures penetrate the low-permeability cap rock (unit B in Fig. 3) and a transient (1–10 yr) connection between the lower (geopressured) and overlying (hydrostatic) fluid reservoirs is established. As fluids move upward in the porous strata, the pressure drops from lithostatic to hydrostatic with consequent boiling, pressure release and fluid removal allowing for subsidence. Afterward, the system, saturated with boiling fluids, begins to seal due to the precipitation of deposited minerals. At this stage, the magma body is restored to its original state before fracturing, except that the H_2O-saturated carapace has migrated to greater depth. In this model there are two timescales; one is the 10^3–10^5 yr timescale associated with magma solidification (and associated magmatic fluid generation). The second timescale (1–10 yr) is intrinsically episodic in nature and associated with transient fracture propagation events (seismicity) that connect the lower lithostatic reservoir with the upper hydrostatic one.

The magmatic–hydrothermal and thermodynamic models proposed here explain available field and laboratory observations, and explain both the periodic ground uplift and subsidence at CF and has predictive implications. According to the model, the magma body is presently isolated from the overlying aquifers and the fraction of exsolved fluid is building within the magma chamber. The next phase of uplift will begin when the rind fractures (seismicity increases), allowing fluid to escape (expulsion from magma) and migrate upward. However, as the magma body cools and crystallizes and the H_2O-saturated carapace migrates to greater depth, the energy and volume change associated with volatile exsolution decreases and the magnitude of future uplift events is likewise expected to decrease. As such, the likelihood of a magmatic eruption at CF is much lower than at any time in the past 500 years, and is expected to continue to decrease. Only if a new batch of magma is emplaced into the subsurface is future volcanic eruption likely.

Acknowledgments

The authors thank Jim Webster and an anonymous reviewer for their comments and suggestions.

Appendix A. Quantitative model for bradyseism

The volume of the magma is a function of the masses and densities of the three phases. That is

$$V(\overline{p},\overline{T}) = \frac{M_s}{\rho_s} + \frac{M_f}{\rho_f} + \frac{M_m}{\rho_m} \tag{1}$$

where M refers to mass of the ith-subscripted phase of density ρ_i. The density of solid, melt and fluid are:

$$\rho_s = \rho_s^o[1-\alpha_s(T_\nearrow - T_s)(\overline{T}-1) + \beta_s p_o(\overline{p}-1)] \tag{2a}$$

$$\rho_m = \rho_m^o\left[1-\alpha_m(T_\nearrow - T_s)(\overline{T}-1) + \beta_m p_o(\overline{p}-1) - \gamma_m a\sqrt{p_o}\left(\sqrt{\overline{p}}-1\right)\right] \tag{2b}$$

$$\rho_f = \frac{\rho_f^o \overline{p} T_\nearrow}{T_\nearrow + \Delta T(\overline{T}-1)} \tag{2c}$$

In Eqs. (2a)–(2c), α is the isobaric expansivity of the subscripted phase, β is the isothermal compressibility of the subscripted phase, γ is a parameter that measures the effect of dissolved water on melt density, $\overline{T}$ is the dimensionless temperature defined as $\overline{T} = \frac{T-T_s}{T_\nearrow - T_s}$, the dimensionless pressure is $\overline{p} = \frac{p}{p_o}$, $\Delta T = T_\nearrow - T_s$ is the liquidus to solidus temperature interval and the constant 'a' relates the solubility of water in the melt to the pressure according to $w^m_{H_2O} = a\sqrt{p_o}\sqrt{\overline{p}}$ where $w_{H_2O}{}^m$ is the mass fraction of water dissolved in the melt and p_o is the initial pressure. The superscript quantities represent the density of each phase at the reference state condition of $T = T_\nearrow$ and $p = p_o$. The mass fraction of water dissolved in the melt (water solubility) at the reference temperature and pressure is $w^o_{H_2O} = a\sqrt{p_o}$. Eq. (2c) assumes ideal gas behavior for H_2O. At pressure less than about 0.5 MPa and magmatic temperatures this is a reasonable approximation. At higher pressure, the ideal gas law predicts too low of a density compared to the real gas. The model could easily be modified to account for the

non-ideal behavior of H_2O by incorporation of a better equation of state for H_2O.

In order to solve Eq. (1), the masses of the various phases must be related to temperature and pressure. The fraction of melt $f_m(\overline{T})$ is taken *a priori* as a monotonically decreasing function of decreasing temperature. A useful parameterization is (Spera and Bohrson, 2001),

$$f_m(\overline{T}) = \frac{L_1}{[1 + \exp(L_2(L_3 - \overline{T}))]^{L_4}}. \quad (3)$$

This form captures the fraction melt–temperature relationship found for fractional or equilibrium (batch) crystallization experimentally and by phase equilibria models such as MELTS (Ghiorso and Sack, 1995). Parameters consistent with melting experiments and from MELTS simulations are $L_1=1$, $L_2=12$, $L_3=0.5$ and $L_4=1$. Alternatively, a simple linear relation such as $f_m(\overline{T})=\overline{T}$ can be imposed. Once f_m is specified, the mass of melt remaining in the magma body as a function of temperature is:

$$M_m = f_m(\overline{T})M_o \quad (4a)$$

The mass of the fluid phase, M_f, is determined assuming H_2O component is partitioned between the melt and coexisting fluid. This assumes that no water is bound in hydrous phases. Because the modal amount of hydrous phases is small and because the mass fraction of water bound in any given hydrous phase is small, this approximation is good. If the total mass fraction of water initially in the system (a constant) is $Z^o_{H_2O}$, then the mass of fluid at any pressure and temperature is

$$M_f = f_f M_o = \left(Z^o_{H_2O} - f_m(\overline{T})a\sqrt{p_o}\sqrt{\overline{p}}\right)M_o \quad (4b)$$

Finally, the mass of solid, M_s is found by mass conservation (i.e., sum of masses is constant equal to M_o). The relation is:

$$M_s = M_o\left[f_m(\overline{T})\left(a\sqrt{p_o}\sqrt{\overline{p}} - 1\right) + 1 - Z^o_{H_2O}\right] \quad (4c)$$

Now if Eqs. (2)–(4) are inserted in Eq. (1), the volume of the system as a function of temperature and pressure is known when constants are fixed and the initial water content of the melt and reference densities are defined. Then one can specify $V=V_o$ in the isochoric case or $p=p_o$ in the isobaric case (open or closed) and solve for the isochoric (P, T) or isobaric (V, T) evolution. The former provides the magma pressure during phase transition whereas the latter provides the volume of the system. In the latter case, there are two branches: one when the system is closed with respect to fluid expulsion (uplift results) and the other when fluids are free to leave the magma and subsidence occurs. In reality, the competition between the rate at which fluid mass is exsolved from melt and that at which it escapes into country rock is critical. It is recognized that this ratio itself can be variable during the protracted evolution of a hydrothermal–magmatic system.

For isochoric crystallization, the pressure–temperature dependant volume equals its initial value, V_o throughout the phase transition. Equality of pressure between all phases means that the pressure of solid, melt and exsolved fluid is identical and identified as the magma pressure, which is computed as a function of temperature. This calculation requires an iterative procedure to solve for pressure as a function of temperature for fixed V_o. Using a reasonable set of parameters, results show that the pressure of the system increases monotonically as the crystallization progresses. The increase in magma pressure is driven by both the density decrease of melt due to increasing dissolved water as pressure increases and because the mass fraction of supercritical fluid increases as the solidus temperature is approached. In this case, because there is no volumetric expansion, i.e., no work (uplift) is done by the crystallizing magma body on its environment. Instead the magma pressure increases. In nature, such a condition leads to fracturing of the wall rock when its strength is exceeded. When this occurs, the isochoric condition no longer holds; then magma continues to lose heat and evolve but now under isobaric conditions.

In isobaric closed system crystallization, the initial pressure is lithostatic (p_o) and constant during phase transition; the volume of the system changes during crystallization and cooling as a function of temperature in order for pressure to remain constant. In this scenario, the wall rocks are not rigid and volume expansion is accommodated by uplift. The system volume $V=V(\overline{p}=1,\overline{T})$ is tracked as a function of temperature. The total pressure–volume work done by the magma in lifting overburden is given by p_o ($V_f - V_o$), where V_f is the final volume of the closed system. The PV work performed by magma volume change is p_o ($V_f - V_o$) and can be either positive (uplift) or negative (subsidence) depending on whether closed or open isobaric conditions apply.

Complex natural systems

The crust into which magma is emplaced beneath CF has heterogeneous thermophysical properties. The precise permeability structure with depth and the degree of permeability anisotropy at CF has not been characterized in detail although it is known that order of magnitude differences in permeability occur between lithological units and that sedimentary layering creates a strong permeability anisotropy. The permeability structure is critical in analysis of hydrothermal flow (e.g., Rosenberg and Spera, 1992; Rosenberg et al., 1993; Schoofs et al., 1999; Schoofs and Spera, 2003; Geiger et al., 2005; Hurwitz et al., 2007a,b). It is also well known that the thermodynamic and transport properties of aqueous geofluids change rapidly and dramatically in regions of pressure–temperature–composition space around the critical point of H_2O (Bodnar and Costain, 1991). The evolution of a natural system can be envisioned as a temporal sequence of states following one or another of the bounding conditions. One sequence of states is phase transition by isochoric pressure build up (no topographic change) followed by wall rock failure with associated isobaric expansion and/or collapse. A key ratio is the mass rate of exsolution of fluid from melt *versus* the rate at which fluid leaks into surrounding country rock of non-zero (but small) permeability. Under isobaric conditions, the rate of fluid exsolution is closely tied to the rate of crystallization which in turn is controlled by the heat exchange rate across the magma–host boundary. The rate of fluid expulsion from the system (into the wall rock) is mainly a function of permeability, which can be highly variable. These coupled processes are intimately related. For example, magmatic heat dissipation leads to thermal cracking in wall rock and that can increase the local permeability. Alternatively, as fluid pressure, initially near the lithostat relaxes to hydrostatic conditions, changes in temperature and pressure will lead to preferential precipitation or dissolution of minerals upon which the permeability depends. The presence of fluid will make more prevalent the possibility of hydrofracture (Shaw, 1980).

References

AGIP, 1987. Geologia e geofisica del sistema geotermico dei Campi Flegrei. Int. Report, p. 17.
Allard, P.A., Maiorani, A., Todesco, D., Cortecci, G., Turi, B., 1991. Isotopic study of the origin of sulfur and carbon in Solfatara fumaroles, Campi Flegrei caldera. J. Volcanol. Geotherm. Res. 48, 139–159.
Aster, R.C., Meyer, R.P., 1988. Three-dimensional velocity structure and hypocenter distribution in the Campi Flegrei caldera, Italy. Tectonophysics 149, 195–218.
Aster, R.C., Meyer, R.P., De Natale, G., Zollo, A., Martini, M., Del Pezzo, E., Scarpa, R., Iannaccone, G., 1992. Seismic investigation of Campi Flegrei Caldera. Volcanic Seismology. Proc.Volcanol. Series, vol. III. Springer Verlag, New York.

Audétat, A., Pettke, T., 1993. The magmatic–hydrothermal evolution of two barren granites: a melt and fluid inclusion study of the Rio del Medio and Canada Pinabete plutons in northern New Mexico (USA). Geochim. Cosmochem. Acta 67, 97–121.
Babbage, C., 1847. Observation on the Temple of Serapis at Pozzuoli near Naples. R. and J. E. Taylor, London. 35 pp.
Battaglia, M., Troise, C., Obrizzo, F., Pingue, F., De Natale, G., 2006. Evidence for fluid migration as the source of deformation at Campi Flegrei caldera (Italy). Geophys. Res. Lett. 33, L01307. doi:10.1029/2005GL024904.
Beane, R.E., Bodnar, R.J., 1995. Hydrothermal fluids and hydrothermal alteration in porphyry copper deposits. Ariz. Geol. Soc. Dig. 20, 83–93.
Beane, R.E., and Titley, S.R., 1981. Porphyry copper deposits. Part II. Hydrothermal alteration and mineralization. Econ. Geol. 75th Anniversary Vol., 235–263.
Bellucci, F., Woo, J., Kilburn, C.R.J., Rolandi, G., 2006. Ground deformation at Campi Flegrei, Italy: implications for hazard assessment. In: Troise, C., De Natale, G., Kilburn, C.R.J. (Eds.), Mechanism of activity and unrest at large calderas: Geol. Soc. London, Spe. Publ., vol. 269, pp. 141–157.
Berrino, G., Gasparini, P., 1995. Ground deformation and caldera unrest. Cah. Cent. Eur. Géodyn. Séismol. 8, 41–55.
Berrino, G., Corrado, G., Luongo, G., Toro, B., 1984. Ground deformation and gravity changes accompanying the 1982 Pozzuoli uplift. Bull. Volcanol. 47, 187–200.
Berrino, G., Rymer, H., Brown, G.C., Corrado, G., 1992. Gravity–height correlation for unrest at calderas. J. Volcanol. Geotherm. Res. 53, 11–26.
Bianchi, R., Cordini, A., Federico, C., Giberti, G., Lanciano, P., Pozzi, J.P., Sartoris, G., Scandone, R., 1987. Modelling of surface ground deformation in volcanic areas: the 1970–1972 and 1982–1984 crises of Campi Flegrei, Italy. J. Geophys. Res. 92 (B13), 14139–14150.
Bodnar, R.J., 1995. Fluid inclusion evidence for a magmatic source for metals in porphyry copper deposits. Miner. Assoc. Can. Short Course 23, 139–152.
Bodnar, R.J., Beane, R.E., 1980. Temporal and spatial variations in hydrothermal fluid characteristics during vein filling in preore cover overlying deeply buried porphyry copper-type mineralization at Red Mountain, Arizona. Ec. Geol. 75, 876–893.
Bodnar, R.J., Costain, J.K., 1991. Effect of fluid composition on mass and energy transport in the earth's crust. Geophys. Res. Lett. 18, 983–986.
Bodnar, R.J., Student, J.J., 2006. Melt inclusions in plutonic rocks: petrography and microthermometry. In: Webster, J.D. (Ed.), Melt inclusions in plutonic rocks: Mineral. Assoc. Canada, Short Course, vol. 36, pp. 1–26.
Bodnar, R.J., Cannatelli, C., De Vivo, B., Lima, A., Belkin, H.E., Milia, A., 2007. Quantitative model for magma degassing and round deformation (bradyseism) at Campi Flegrei, Italy: implications for future eruptions. Geology 35 (9), 791–794. doi:10.1130/G23653A.1.
Bonafede, M., 1990. Axi-symmetric deformation of a thermo-poro-elastic half-space: inflation of a magma chamber. Geophys. Int. 103.
Bonafede, M., 1991. Hot fluid migration: an efficient source of ground deformation. Application to the 1982–85 crisis at Campi Flegrei, Italy. In: Luongo, G., Scandone, R. (Eds.), Campi Flegrei: J. Volcanol. Geotherm. Res., vol. 48, pp. 187–198.
Bonafede, M., Dragoni, M., Quareni, F., 1986. Displacement and stress fields produced by a centre of dilatation and by a pressure source in visco-elastic half-space: application to the study of ground deformation and seismic activity at Campi Flegrei, Italy. Geophys. J. R. Astron. Soc. 87, 455–485.
Bredeholft, J.D., Hanshaw, B.B., 1968. On the maintenance of anomalous fluid pressures: I. Thick sedimentary sequences. Geol. Soc. Am. Bull. 79, 1097–1106.
Breislak, S., 1792. Essai mineralogiques sur le Solfatare de Pouzzole. Part 3, Observations sur l'exterieur du crater de la Solfatare. Giaccio, Naples, pp. 170–177.
Burnham, C.W., 1972. The energy of explosive volcanic eruptions. Earth Miner. Sci., Pa. State Univ. 41, 69–70.
Burnham, C.W., 1985. Energy release in subvolcanic environments: implications for breccia formation. Econ. Geol. 80, 1515–1522.
Burnham, C.W., Holloway, J.R., Davis, N.F., 1969. Thermodynamic properties of water to 1000 °C and 10,000 bars. Geol. Soc. Am. Spec. Pap. 132, 96.
Caliro, S., Chiodini, G., Moretti, R., Avino, R., Granieri, D., Russo, M., Fiebig, J., 2007. The origin of the fumaroles of La Solfatara (Campi Flegrei, South Italy). Geochim. Cosmochem. Acta 71 (12), 3040–3055. doi:10.1016/j.gca.2007.04.007.
Casertano, L., Oliveri del Castillo, A., Quagliariello, M.T., 1976. Hydrodynamics and geodynamics in the Phlegraean Fields area of Italy. Nature 264, 154–161.
Chiodini, G., Todesco, M., Caliro, S., Del Gaudio, C., Macedonio, G., Russo, M., 2003. Magma degassing as a trigger of bradyseismic events: the case of Phlegrean Fields, Italy. Geophys. Res. Lett. 30, 1434. doi:10.1029/2002GLO16790.
Cline, J.S., Bodnar, R.J., 1994. Direct evolution of a brine from a crystallizing silicic melt at the Questa, New Mexico, molybdenum deposit. Econ. Geol. 89, 1780–1802.
Corrado, G., Guerra, I., Lo Bascio, A., Luongo, G., Rampoldi, F., 1976. Inflation and microearthquake activity of Phlegraean Fields, Italy. Bull. Volcanol. 40 (3), 169–188.
Cortini, M., Barton, C.C., 1993. Non linear forecasting analysis of inflation–deflation patterns of an active caldera (Campi Flegrei, Italy). Geology 21, 239–242.
Cortini, M., Cilento, L., Rullo, A., 1991. Vertical ground movements in the Campi Flegrei caldera as a chaotic dynamic phenomenon. J. Volcanol. Geotherm. Res. 48, 103–114.
Cubellis, E., Di Donna, G., Luongo, G., Mazzarella, A., 2002. Simulating the mechanism of magmatic processes in the Campi Flegrei area (southern Italy) by the Lorenz equations. J. Volcanol. Geotherm. Res. 115, 339–349.
De Natale, G., Pingue, F., Allard, P., Zollo, A., 1991. Geophysical and geochemical modeling of the Campi Flegrei caldera. In: Luongo, G., Scandone, R. (Eds.), Campi Flegrei. J. Volcanol. Geotherm. Res., 48, pp. 199–222.
De Natale, G., Zollo, A., Ferraro, A., Virieux, J., 1995. Accurate fault mechanism determinations for a 1984 earthquake swarm at Campi Flegrei caldera (Italy) during an unrest episode: implications for volcanological research. J. Geophys. Res. 100 (B12), 24167–24185.
De Natale, G., Troise, C., Pingue, F., 2001. A mechanical fluid-dynamical model for ground movements at Campi Flegrei caldera. J. Geodyn. 32, 487–517.
De Vivo, B., Lima, A., 2006. A hydrothermal model for ground movements (bradyseism) at Campi Flegrei, Italy. In: De Vivo, B. (Ed.), Volcanism in the Campania Plain. Vesuvius, Campi Flegrei, Ignimbrites Developments in Volcanology, vol. 9. Elsevier, pp. 289–317.
De Vivo, B., Belkin, H.E., Barbieri, M., Chelini, W., Lattanzi, P., Lima, A., Tolomeo, L., 1989. The Campi Flegrei (Italy) geothermal system: a fluid inclusion study of the Mofete and San Vito fields. J. Volcanol. Geotherm. Res. 36, 303–326.
De Vivo, B., Torok, K., Ayuso, R.A., Lima, A., Lirer, L., 1995. Fluid inclusion evidence for magmatic/saline/CO_2 immiscibility and geochemistry of alkaline xenoliths from Ventotene Island, Italy. Geochim. Cosmochim. Acta 59 (14), 2941–2953.
De Vivo, B., Lima, A., Webster, J.D., 2005. Volatiles in magmatic–volcanic systems. Elements 1, 19–24.
De Vivo, B., Lima, A., Kamenetsky, V.S., Danyushevsky, L.V., 2006. Fluid and melt inclusions in the sub-volcanic environments from volcanic systems: examples from the Neapolitan area and Pontine islands (Italy). In: Webster, J.D. (Ed.), Melt Inclusions in Plutonic Rocks: Min. Ass. of Canada Short Course, Montreal, Quebec, vol. 36. ISBN: 0-921294-36-0, pp. 211–237.
Del Gaudio, C., Ricco, C., Equino, I., Brandi, G., Serio, C., Siniscalchi, V., 2005. Misure di livellazione di precisione e dati tiltmetrici per il controllo delle deformazioni del suolo ai Campi Flegrei. INGV-OSSERVATORIO VESUVIANO. Open File Report http://www.ov.ingv.it.
Dvorak, J.J., Gasparini, P., 1991. History of earthquakes and vertical ground movement in Campi Flegrei caldera, Southern Italy: comparison of precursory events to the A. D. 1538 eruption of Monte Nuovo and of activity since 1968. J. Volcanol. Geotherm. Res. 48, 77–92.
Dvorak, J.J., Mastrolorenzo, G., 1991. The mechanism of recent vertical crustal movements in Campi Flegrei caldera, Southern Italy. Geol. Soc. Am. Spec. Pap. 263.
Dzurisin, D., Savage, J.C., Fournier, R.O., 1990. Recent crustal subsidence at Yellowstone Caldera, Wyoming. Bull. Volcanol. 52, 247–270.
Esposito, R., Bodnar, R.J., De Vivo, B., Lima, A., Fedele, L., Shimizu, N., Belkin, H.E., Hunter, J., 2009a. Volatile evolution of magma associated with the Solchiaro eruption in the Phlegrean volcanic District. AGU Spring Meeting, Toronto, Canada.
Esposito, R., Bodnar, R.J., De Vivo, B., Lima, A., Fedele, L., Shimizu, N., Belkin, H.E., Hunter, J., 2009b. Volatile evolution of magma associated with the Solchiaro eruption in the Phlegrean volcanic District. ECROFI XX, Granada, Spain.
Faccenna, C., Funiciello, F., Giardini, D., Lucente, P., 2001. Episodic back-arc extension during restricted mantle convection in the central Mediterranean. Earth Planet. Sci. Lett. 187, 105–116.
Ferrucci, F., Hirn, A., Virieux, J., De Natale, G., Mirabile, L., 1992. P-SV conversions at a shallow boundary beneath Campi Flegrei caldera (Naples, Italy): evidence for the magma chamber. J. Geophys. Res. 97 (B11), 15351–15359.
Forbes, J.D., 1829. Physical notice in the Bay of Naples. Number 5, on the temple of Jupiter Serapis at Pozzuoli and the phenomena which it exhibits. Edin. J. Sci. New Ser. 1, 260–286.
Foulger, G.R., Julian, B.R., Pitt, A.M., Hill, D.P., Malin, P.E., Shalev, E., 2003. Three-dimensional crustal structure of Long Valley caldera, California, and evidence for the migration of CO_2 under Mammoth Mountain. J. Geophys. Res. 108, 2147–2163.
Fournier, R.O., 1989. Geochemistry and dynamics of the Yellowstone National Park hydrothermal system. Annu. Rev. Earth Planet. Sci. 17, 13–53.
Fournier, R.O., 1999. Hydrothermal processes related to movement of fluid from plastic into brittle rock in the magmatic–epithermal environment. Econ. Geol. 94 (8), 1193–1212.
Fowler, S.J., Spera, F.J., Bohrson, W.A., Belkin, H.E., De Vivo, B., 2007. Phase equilibria constraints on the chemical and physical evolution of the Campanian ignimbrite. J. Petrol. 48, 459–493.
Gaeta, F.S., Peluso, F., Arienzo, I., Castagnolo, D., De Natale, G., Milano, G., Albanese, C., Mita, D.G., 2003. A physical appraisal of a new aspect of bradyseism: the miniuplifts. J. Geophys. Res. 108 (8), 2363. doi:10.1029/2002JB001913.
Geiger, S., Driesner, T., Heinrich, C.A., Matthaei, S.K., 2005. On the dynamics of NaCl–H (sub 2) O fluid convection in the Earth's crust. J. Geophys. Res. 110 (B7), 23.
Ghiorso, M.S., Sack, R.O., 1995. Chemical mass transfer in magmatic processes. IV. A revised and internally consistent thermodynamic model for the interpolation and extrapolation of liquid–solid equilibria in magmatic systems at elevated temperatures and pressures. Contrib. Mineral. Petrol. 119, 197–212.
Goes, S., Giardini, D., Jenny, S., Hollenstein, C., Kahle, H.G., Geiger, A., 2004. A recent tectonic reorganization in the south-central Mediterranean. Earth Planet. Sci. Lett. 226, 335–345.
Guidarelli, M., Saraò, A., Panza, G.F., 2002. Surface wave tomography and seismic source studies at Campi Flegrei (Italy). Phys. Earth Planet. Inter. 134, 157–173.
Guidarelli, M., Zille, A., Saraò, A., Natale, M., Nunziata, C., Panza, G.F., 2006. Shear-wave velocity models and seismic sources in Campanian volcanic areas: Vesuvius and Phlegraean Fields. In: Dobran, F. (Ed.), VESUVIUS 2000: Education, Security and Prosperity. Elsevier, pp. 287–309.
Gunther, R.T., 1903. The submerged Greek and Roman foreshore near Naples. Archaeologia 58, 62.
Hill, D.P., Pollitz, F., Newhall, C., 2002. Earthquake–volcano interactions. Physics Today, November, pp. 41–47.
Huppert, H.E., Woods, A.W., 2002. The role of volatiles in magma chamber dynamics. Nature 420, 493–495.
Hurwitz, S., Lowenstern, J.B., Heasler, H., 2007a. Spatial and temporal geochemical trends in the hydrothermal system of Yellowstone National Park: influences from river solute flux. J. Volcanol. Geotherm. Res. 162, 149–171. doi:10.1016/j.volgeores.2007.01.003.
Hurwitz, S., Christiansen, L.B., Hsieh, P.A., 2007b. Hydrothermal fluid flow and deformation in large calderas: influences from numerical simulations. J. Geophys. Res. 112, B02206. doi:10.1029/2006JB004689 16 pp.

Kostrov, B.V., Das, S., 1988. Principles of Earthquake Source Mechanics. Cambridge Univ. Press. Cambridge, U.K, Cambridge. 286 pp.
Lange, R.A., 1994. The effect of H_2O and CO_2 on the density and viscosity of silicate melts. In: Ribbe, P.H. (Ed.), Volatiles in Magmas: Reviews in Mineralogy, vol. 30, pp. 331–370.
Lange, R.A., Carmichael, I.S.E., 1990. Thermodynamic properties of silicate liquids with emphasis on density, thermal expansion and compressibility. In: Nicolls, J., Russell, J.K. (Eds.), Modern Methods of Igneous Petrology: Understanding Magmatic Processes. Reviews in Mineralogy, vol. 24, pp. 25–64.
Lowenstern, J.B., Hurwitz, S., 2007. Monitoring a supervolcano in repose: heat and volatile flux at the Yellowstone caldera. Elements 4, 35–40.
Lyell, C., 1872. In: Murray, J. (Ed.), Principles of Geology. London, pp. 164–179.
Macedonio, G., Tammaro, U., 2005. Attività di Sorveglianza dell'Osservatorio Vesuviano. Rendiconto anno 2003. INGV-OSSERVATORIO VESUVIANO. http://www.ov.ingv.it/.
Martini, M., Giannini, L., Buccianti, A., Prati, F., Legittimo, P.C., Bozzelli, P., Capaccioni, B., 1991. 1980–1990: ten years of geochemical investigation at Phlegrean Fields (Italy). J. Volcanol. Geotherm. Res. 48, 161–171.
McGarr, A., 1976. Seismic moments and volume changes. J. Geophys. Res. 81, 14871494.
McKibben, R., Tyvand, P.A., 1982. Anisotropic modeling of thermal convection in multilayered porous media. J. Fluid Mech. 118, 315–339.
Milia, A., Torrente, M.M., 1999. Tectonics and stratigraphic architecture of a pery-Tyrrhenian half-graben (Bay of Naples Italy). Tectonophysics 315, 297–314.
Milia, A., Torrente, M.M., 2000. Fold uplift and syn-kinematic stratal architectures in a region of active transtensional tectonics and volcanism, Eastern Tyrrhenian Sea. Geol. Soc. Am. Bull. 112, 1531–1542.
Milia, A., Torrente, M.M., 2003. Late Quaternary Volcanism and transtensional tectonics in the Bay of Naples, Campanian continental margin, Italy. Miner. Petrol. 79, 49–65.
Milia, A., Torrente, M.M., 2007. The influence of paleogeographic setting and crustal subsidence on the architecture of ignimbrites in the Bay of Naples (Italy). Earth Planet. Sci. Lett. 263, 192–206.
Milia, A., Torrente, M.M., Giordano, F., 2000. Active deformation and volcanism offshore Campi Flegrei, Italy: new data from high resolution seismic reflection profiles. Mar. Geol. 171, 61–73.
Milia, A., Torrente, M.M., Russo, M., Zuppetta, A., 2003. Tectonics and crustal structure of the Campania continental margin: relationships with volcanism. Miner. Petrol. 79, 33–47.
Milia, A., Torrente, M.M., Giordano, F., Mirabile, L., 2006. Rapid changes of the accommodation space in the Late Quaternary succession of Naples Bay, Italy: the influence of volcanism and tectonics. In: De Vivo, B. (Ed.), Volcanism in the Campania Plain: Vesuvius, Campi Flegrei and Ignimbrites. Series "Developments in Volcanology", vol. 9. Elsevier, pp. 53–68.
Mogi, K., 1958. Relations between the eruptions of various volcanoes and the deformations of the ground surfaces around them. Bull. Earthq. Res. Inst. Univ. Tokyo 36, 99–134.
Morhange, C., Marriner, N., Laborel, J., Todesco, M., Oberlin, C., 2006. Rapid sea level movements and noneruptive crustal deformations in the Phlegrean Fields caldera, Italy. Geology 34, 93–96.
Neuzil, C.E., 1995. Abnormal pressures as hydrodynamic phenomena. Am. J. Sci. 295, 742–786.
Niccolini, A., 1839. Tavola cronologica-metrica delle varie altezze tracciate dal mare fra la costa di Amalfi ed il promontorio di Gaeta nel corso di diaciannove secoli. Flautina, Napoli, pp. 11–52.
Niccolini, A., 1845. Descrizione della gran terna puteolana volgarmente detta Tempio di Se rapide. Napoli, Stamperia Reale.
Nunziata, C., submitted for publication. Average shear wave velocity models of the crustal structure in the Neapolitan area, between Campi Flegrei and Vesuvio volcanic areas. Phys. Earth Planet. Inter.
Oliveri del Castillo, A., Quagliariello, M.T., 1969. Sulla genesi del bradisismo flegreo. Atti Associazione Geofisica Italiana, 18th Congress, Napoli, pp. 557–594.
Panichi, C., Volpi, G., 1999. Hydrogen, oxygen and carbon isotope ratios of solfatara fumaroles (Phlegraean Fields, Italy): further insights into source processes. J. Volcanol. Geotherm. Res. 91, 321–328.
Panza, G.F., Pontevivo, A., Saraò, A., Aoudia, A., Peccerillo, A., 2004. Structure of the lithosphere–asthenosphere and volcanism in the Tyrrhenian Sea and surroundings. From Seafloor to Deep Mantle: Architecture of the Tyrrhenian Backarc Basin. In: Marani, et al. (Ed.), Mem. Descr. Carta Geologica d'Italia, vol. 64, pp. 29–56.
Panza, G.F., Peccerillo, A., Audia, A., Farina, A., 2007. Geophysical and petrological modelling of the structure and composition of the crust and upper mantle in complex of geodynamic setting: the Thyrrenian Sea and surrounding. Earth-Sci. Rev. 80, 1–46.
Parascandola, A., 1947. I fenomeni bradisismici del Serapeo di Pozzuoli, Napoli. Privately published, 156 pp.
Pierce, K.L., Cannon, K.P., Meyer, G.A., Trebesch, M.J., Watts, R., 2002. Post-glacial inflation–deflation cycles, tilting and faulting in the Yellowstone caldera based on Yellowstone lake shorelines. U.S. Geological Survey Open-File Report 02-0142.
Pingue, F., De Martino, P., Obrizzo, F., Serio, C., Tammaro, U., 2006. Stima del campo di spostamento ai Campi Flegrei da dati CGPS e di livellazione di precisione nel periodo maggio 2004 - marzo 2006. INGV-OSSERVATORIO VESUVIANO. Open File Report http://www.ov.ingv.it.
Roedder, E., Bodnar, R.J., 1997. Fluid inclusion studies of hydrothermal ore deposits, In: Barnes, H.L. (Ed.), Geochemistry of Hydrothermal Ore Deposits, 3rd Ed. Wiley and Sons, New York, pp. 657–698.
Rosenberg, N., Spera, F.J., 1992. Thermohaline convection in a porous medium heated from below. Int. J. Heat Mass Transfer 35, 1261–1274.
Rosenberg, N., Spera, F.J., Haymon, R., 1993. The relationship between flow and permeability field in seafloor hydrothermal systems. Earth Planet. Sci. Lett. 116, 135–153.
Rosi, M., Sbrana, A. (Eds.), 1987. Phlegrean Fields, 114 Consiglio Nazionale delle Ricerche, Roma, pp. 1–175.
Saccorotti, G., Petrosino, S., Bianco, F., Castellano, M., Galluzzo, D., La Rocca, M., Del Pezzo, E., Maccarelli, L., Cusano, P., 2007. Seismicity associated with the 2004–2006 renewed ground uplift at Campi Flegrei Caldera, Italy. Phys. Earth Planet. In. 165, 14–24.
Sartori, R., 2003. The Tyrrhenian back-arc basin and subduction of the Ionian lithosphere. Episodes 26, 217–221.
Sasada, M., 2000. Igneous-related active geothermal system versus porphyry copper hydrothermal system. Proceeding World Geothermal Congress 2000, Kyushu–Tohoku, Japan, May 28–June 10, pp. 1691–1693.
Schoofs, S., Spera, F.J., 2003. Transition to chaos and flow dynamics of thermochemical porous medium convection. Transp. Porous Med. 50, 179–195.
Schoofs, S., Spera, F.J., Hansen, U., 1999. Chaotic thermohaline convection in low-porosity hydrothermal systems. Earth Planet. Sci. Lett. 174, 213–229.
Shaw, H.R., 1980. The fracture mechanisms of magma transport from the mantle to the surface. In: Hargraves, R.B. (Ed.), The Physics of Magmatic Processes: Princeton. New Jersey, Princeton University Press, pp. 201–264.
Sibson, R.H., 2003. Brittle-failure controls on maximum sustainable overpressure in different tectonic regimes. AAPG Bull. 87, 901–908.
Spera, F.J., 1981. Carbon dioxide in petrogenesis II. Fluid dynamics of mantle metasomatic processes. Contr. Mineral. Petrol. 77, 56–65.
Spera, F.J., Bohrson, W.A., 2001. Energy-constrained open-system magmatic processes I: general model and energy-constrained assimilation and fractional crystallization (EC-AFC) formulation. J. Petrol. 42, 999–1018.
Spera, F.J., Bohrson, W.A., Till, Christy, B., Ghiorso, M.S., 2007. Partitioning of trace elements among coexisting crystals, melt, and supercritical fluid during isobaric crystallization and melting. Am. Mineral. 92, 1881–1898.
Tait, S., Jaupart, C., Vergniolle, S., 1989. Pressure, gas content and eruption periodicity of a shallow crystallizing magma chamber. Earth Planet. Sci. Lett. 92, 107–123.
Todesco, M., Berrino, G., 2005. Modeling hydrothermal fluid circulation and gravity signals at the Phlegrean Fields caldera. Earth Planet. Sci. Lett. 240, 328–338.
Todesco, M., Scarsi, P., 1999. Chemical (He, H_2, CH_4, Ne, Ar, N_2) and isotopic (He, Ne, Ar, C) variations in the Solfatara crater (southern Italy): mixing of different sources in relation to seismic activity. Earth Planet. Sci. Lett. 171, 465–480.
Todesco, M., Chiodini, G., Macedonio, G., 2003. Monitorino and modeling hydrothermal fluid emission at La Solfatara (Phlegrean Fields, Italy). An interdisciplinary approach to the study of diffuse degassing. J. Volcanol. Geotherm. Res. 125, 57–79.
Todesco, M., Rutqvist, J., Chiodini, G., Pruess, K., Oldenburg, C.H., 2004. Modeling of recent volcanic episodes at Phlegrean Fields (Italy): geochemical and ground deformation. Geothermics 33, 531–547.
Trasatti, E., Giunchi, G., Bonafede, M., 2005. Structural and rheological constraints on source depth and overpressure estimate at the Campi Flegrea caldera, Italy. J. Volcanol. Geotherm. Res. 144, 105–118.
Trasatti, E., Casu, F., Giunchi, C., Pepe, S., Solaro, G., Tagliaventi, S., Berardino, P., Manzo, M., Pepe, A., Ricciardi, G.P., Sansosti, E., Tizzani, P., Zeni, G., Lanari, R., 2008. The 2004–2006 uplift episode at Campi Flegrei caldera (Italy): constraints from SBAS-DInSAR ENVISAT data and Bayesian source inference. Geophys. Res. Lett. 35, L07308. doi:10.1029/2007GL033091.
Troise, C., De Natale, G., Pingue, F., Obrizzo, F., De Martino, P., Tammaro, U., Boschi, E., 2007. Renewed ground uplift at Campi Flegrei caldera (Italy): new insight on magmatic processes and forecast. Geophys. Res. Lett. 34, L03301. doi:10.1029/2006GL028545.
Turco, E., Schettino, A., Pierantoni, P.P., Santarelli, G., 2006. The Pleistocene extension of the Campania Plain in the frame work of the southern Tyrrhenian tectonic evolution: morphotectonic analysis, kinematic model and implications for volcanism. In: De Vivo (Ed.), Volcanism in the Campania Plain: Vesuvius, Campi Flegrei and Ignimbrites. Series Developments in Volcanology, vol. 9. Elsevier, pp. 27–51.
Vilardo, G., Alessio, G., Luongo, G., 1991. Analysis of the magnitude–frequency distribution for the 1983–1984 earthquake activity of Campi Flegrei, Italy. J. Volcanol. Geotherm. Res. 48, 115–125.
Wallis, G.B., 1969. One Dimensional Two-Phase Flow. New York, McGraw-Hill. 408 pp.
Walther, J.V., Helgeson, H.C., 1977. Calculation of the thermodynamic properties of aqueous silica and the solubility of quartz and its polymorphs at high pressures and temperatures. Am. J. Sci. 277, 1315–1351.
Wood, S.A., Spera, F.J., 1984. Adiabatic decompression of aqueous solutions: applications to hydrothermal fluid migration in the crust. Geology 12, 707–710.
Woods, A.W., Huppert, H.E., 2003. On magma chamber evolution during slow effusive eruptions. J. Geophys. Res. 108 ECV 12-1-ECV 12-16.
Wortel, M., Spakman, W., 2000. Subduction and slab detachment in the Mediterranean–Carpathian Region. Science 290, 1910–1917.
Yokoyama, I., 2006. The 1969–1985 Pozzuoli event and active volcanisms. Proc. Jpn. Acad., Ser. B 82, 121–126.
Yokoyama, I., Nazzaro, A., 2002. Anomalous crustal movements with low seismic efficiency — Campi Flegrei, Italy and some examples in Japan. Ann. Geophys. 45, 709–722.
Zollo, A., Maercklin, N., Vassallo, M., Dello Iacono, D., Virieux, J., Gasparini, P., 2008. Seismic reflections reveal a massive melt layer feeding Campi Flegrei caldera. Geophys. Res. Lett. 35, L12306. doi:10.1029/2008GL034242.
Zuppetta, A., Sava, A., 1991. Stress pattern at Campi Flegrei from focal mechanisms of the 1982–1984 earthquakes (Southern Italy). J. Vocanol. Geotherm. Res. 48, 127–137.